US011554345B2

(12) **United States Patent**
Patrick

(10) **Patent No.: US 11,554,345 B2**
(45) **Date of Patent: Jan. 17, 2023**

(54) PROCESS AND APPARATUS TO REMOVE CARBON-14 FROM CARBON-DIOXIDE IN ATMOSPHERIC GASES AND AGRICULTURAL PRODUCTS GROWN IN CONTROLLED ENVIRONMENTS

(71) Applicant: **Brett Evan Patrick**, Grants Pass, OR (US)

(72) Inventor: **Brett Evan Patrick**, Grants Pass, OR (US)

(73) Assignee: **Brett Patrick**, Grants Pass, OR (US)

(*) Notice: Subject to any disclaimer, the term of this patent is extended or adjusted under 35 U.S.C. 154(b) by 0 days.

(21) Appl. No.: **17/540,687**

(22) Filed: **Dec. 2, 2021**

(65) **Prior Publication Data**

US 2022/0161191 A1 May 26, 2022

Related U.S. Application Data

(60) Continuation of application No. 17/159,517, filed on Jan. 27, 2021, now Pat. No. 11,192,067, which is a
(Continued)

(51) **Int. Cl.**
B04C 5/04 (2006.01)
B01D 59/20 (2006.01)
(Continued)

(52) **U.S. Cl.**
CPC ***B01D 59/20*** (2013.01); ***A01G 7/02*** (2013.01); ***B04C 5/04*** (2013.01); ***B04C 5/081*** (2013.01);
(Continued)

(58) **Field of Classification Search**
CPC B01D 59/20; B01D 2258/05; A01G 7/02; B04C 5/04; B04C 5/081; B04C 5/14; B04C 5/181; B04C 2009/005; G21C 19/303
See application file for complete search history.

(56) **References Cited**

U.S. PATENT DOCUMENTS

1,344,146 A * 6/1920 Peck B04C 1/00
209/722
1,798,510 A * 3/1931 Winslow F02M 35/022
55/459.3
(Continued)

OTHER PUBLICATIONS

Feiverson, H. A., Glaser, A., Mian, Z., & Von Hippel, F. N., Unmaking the Bomb: A Fissile Material Approach to Nuclear Disarmament and Nonproliferation, The MIT Press, Cambridge, Massachusetts, London, England (2014).

Genome Reference Consortium (GRC) Human Genome Assembly build 38 (GRCh38), Dec. 24, 2013, 4 pages.

(Continued)

Primary Examiner — Dung H Bui

(74) *Attorney, Agent, or Firm* — Chernoff, Vilhauer, McClung & Stenzel, LLP

(57) ABSTRACT

This invention relates to a process and apparatus for growing agricultural products with a reduced abundance of radioactive carbon-14 (^{14}C) by employing centrifugal separation of atmospheric gases to selectively remove carbon dioxide (CO_2) with ^{14}C. Agricultural products with reduced ^{14}C content can be grown in controlled environments with filtered atmospheric gases for the benefit of reducing harmful damage to human DNA that is unavoidable with our current food chain, due to the natural abundance of ^{14}C in atmospheric gases. Bilateral and unilateral compression helikon vortex apparatus provide efficient and economical removal of CO_2 with ^{14}C from atmospheric gases with a single filtration pass, which is ideally suited for large scale agricultural production.

7 Claims, 17 Drawing Sheets

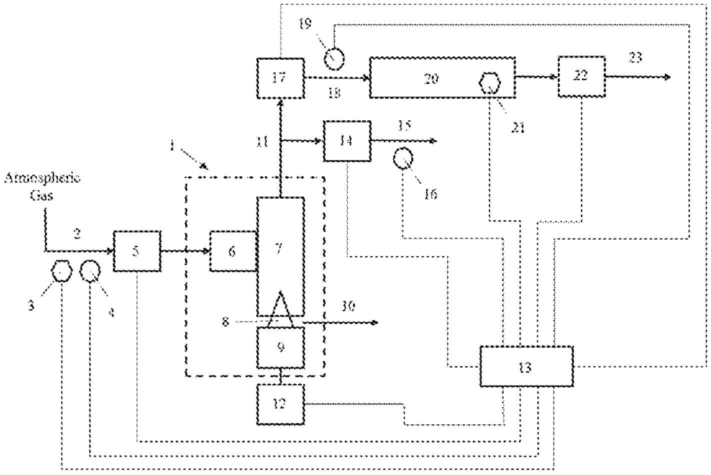

Related U.S. Application Data

division of application No. 16/030,734, filed on Jul. 9, 2018, now Pat. No. 10,905,998.

(60) Provisional application No. 62/535,211, filed on Jul. 20, 2017.

(51) **Int. Cl.**

A01G 7/02	(2006.01)
B04C 5/081	(2006.01)
B04C 5/181	(2006.01)
B04C 5/14	(2006.01)
B04C 9/00	(2006.01)
G21C 19/303	(2006.01)

(52) **U.S. Cl.**

CPC ***B04C 5/14*** (2013.01); ***B04C 5/181*** (2013.01); *B01D 2258/05* (2013.01); *B04C 2009/005* (2013.01); *G21C 19/303* (2013.01)

(56) **References Cited**

U.S. PATENT DOCUMENTS

1,985,947	A	*	1/1935	O'Mara	B04C 5/14 55/432
2,033,471	A	*	3/1936	Josephh	B04C 5/04 209/722
2,681,124	A	*	6/1954	Der Kolk	B04C 5/14 210/512.1
2,781,910	A	*	2/1957	Fontein	B01D 17/0217 210/252
2,927,693	A		3/1960	Freeman et al.	
3,004,158	A		10/1961	Steimel	
3,129,173	A	*	4/1964	Schulze	B04C 5/04 210/512.1
3,421,334	A		1/1969	McKinney et al.	
3,594,573	A		7/1971	Greber	
3,745,752	A		7/1973	Gallaer	
3,766,661	A		10/1973	Bayens et al.	
3,802,570	A		4/1974	Dehne	
3,850,816	A		11/1974	Koch	
3,925,036	A		12/1975	Shacter	
3,928,186	A		12/1975	Zemanek	
3,939,354	A		2/1976	Janes	
3,942,975	A		3/1976	Drummond et al.	
3,989,485	A		11/1976	Killian	
3,990,634	A		11/1976	Hejlek	
4,005,998	A		2/1977	Gorman	
4,070,171	A		1/1978	Wikdahl	
4,311,674	A		1/1982	Janner et al.	
4,317,716	A		3/1982	Liller	
4,578,199	A		3/1986	Peel et al.	
4,584,073	A		4/1986	Lahoda et al.	
4,638,674	A		1/1987	Redmann	
4,670,161	A		6/1987	Hayatdavoudi	
4,692,311	A		9/1987	Parker et al.	
4,816,209	A		3/1989	Schweiger	
4,842,145	A		6/1989	Boadway	
4,848,993	A		7/1989	Elkjaer	
4,865,633	A		9/1989	Stevenson	
5,071,557	A		12/1991	Schubert et al.	
5,106,514	A		4/1992	Alexander	
5,566,835	A		10/1996	Grimes	
5,771,844	A		6/1998	Dietz	
6,036,027	A		3/2000	Grimes	
6,530,484	B1		3/2003	Bosman	
6,596,169	B1		7/2003	Rong et al.	
7,332,715	B2		2/2008	Russ, IV et al.	
8,192,614	B2		6/2012	Niccum et al.	
8,460,434	B2		6/2013	Turner et al.	
9,579,666	B2		2/2017	Mangadoddy et al.	
2007/0068127	A1	*	3/2007	Noguchi	B04C 5/28 55/459.1
2007/0131594	A1		6/2007	Hakola	
2009/0294384	A1	*	12/2009	Kruyer	B04C 5/04 210/151
2010/0255975	A1	*	10/2010	Mauchle	B04C 5/14 494/23
2010/0313751	A1	*	12/2010	Hassan	B04B 7/08 95/45
2012/0285322	A1		11/2012	Halpap et al.	
2013/0239816	A1		9/2013	Mantilla et al.	
2016/0089626	A1	*	3/2016	Kilian	B01D 53/1418 96/253
2018/0236397	A1	*	8/2018	Baxter	B04C 5/08
2018/0238620	A1	*	8/2018	Baxter	F25J 3/0655

OTHER PUBLICATIONS

Lander, E. S. et al., "Initial sequencing and analysis of the human genome", Nature 409, Feb. 15, 2001, pp. 860-921.

Moore, J. D. L., South Africa and Nuclear Proliferation, Palgrave Macmillan, New York, NY (1987).

Patrick, A. D., & Patrick, B. E., "Carbon 14 decay as a source of somatic point mutations in genes correlated with cancer diagnoses", Stable Isotope Foundation, Grants Pass, Oregon, USA, 2017, 81 pages.

Purdom, C. E., "Biological hazards of carbon-14", New Sci. 298, Aug. 2, 1962, pp. 255-257.

Sassi, M., et al., "Carbon-14 decay as a source of non-canonical bases in DNA", Biochimica et Biophysica Acta 1840, 2014, pp. 526-534.

Sender, R., Fuchs, S., & Milo, R., "Revised estimates for the number of human and bacteria cells in the body", PLoS Biol 14(8): e1002533, Aug. 19, 2016, 14 pages.

Office Action prepared by the US Patent and Trademark Office for U.S. Appl. No. 16/030,734, filed Apr. 24, 2020, 7 pages.

Office Action prepared by the US Patent and Trademark Office for U.S. Appl. No. 16/030,734, filed May 21, 2020, 12 pages.

* cited by examiner

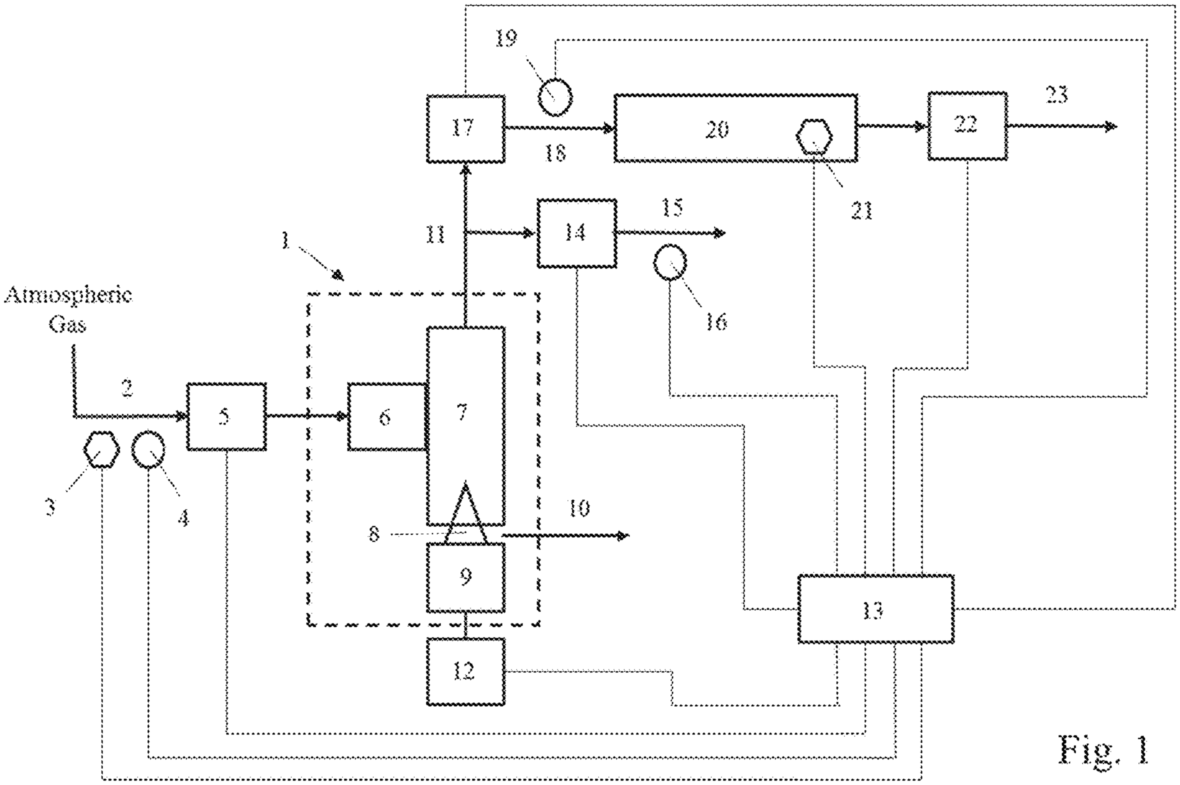
19
17
18
20
21
22
23
1
11
14
15
16
Atmospheric Gas
2
5
6
7
3
4
8
10
9
13
12

Fig. 1

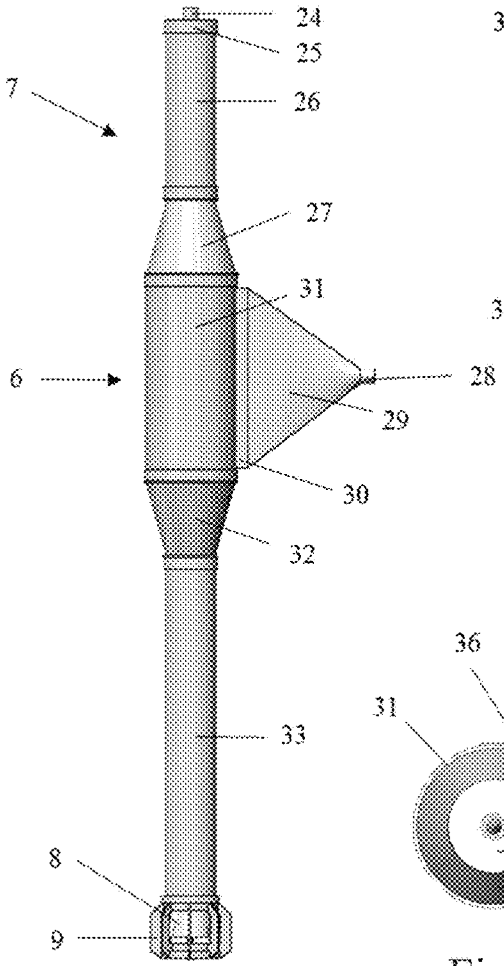

Fig. 2A

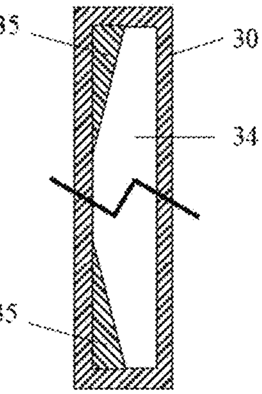

Fig. 2D

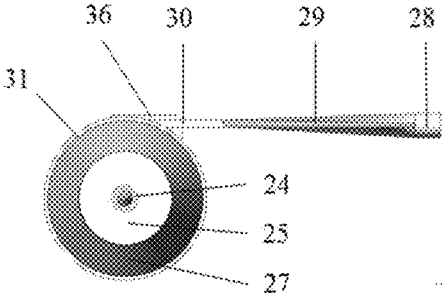

Fig 2B

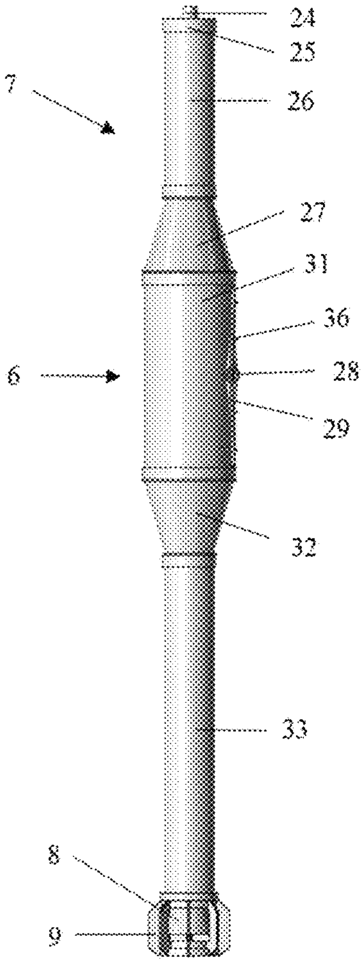

Fig. 2C

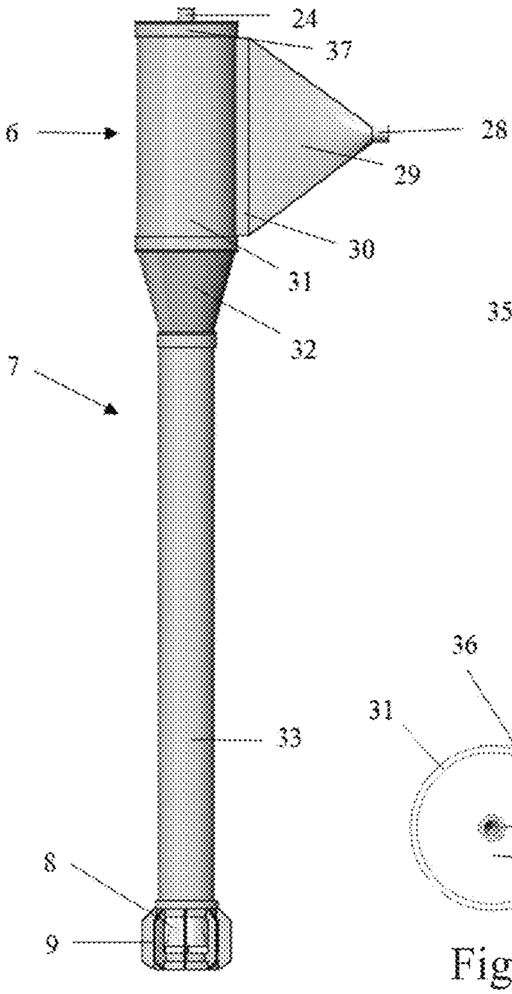

Fig. 3A

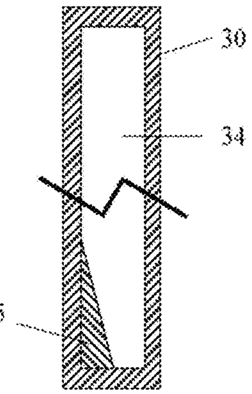

Fig. 3D

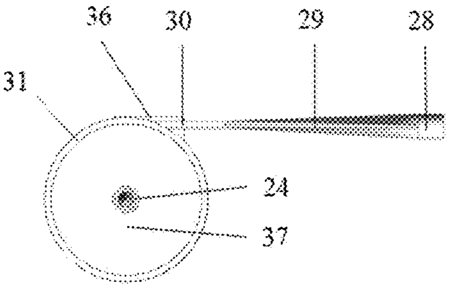

Fig. 3B

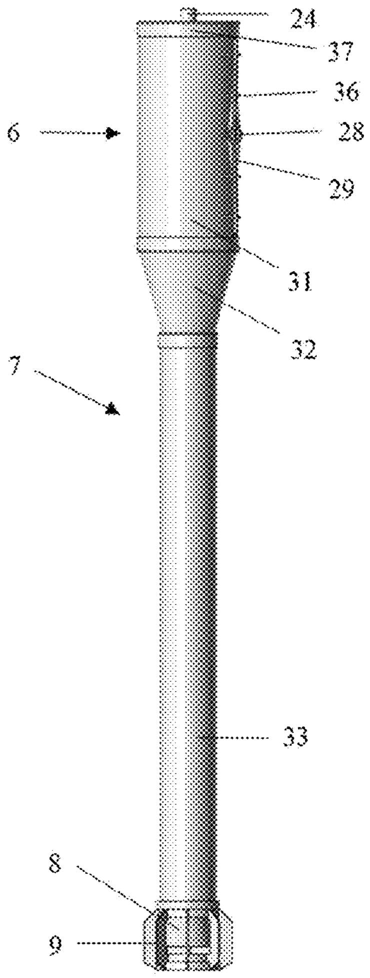

Fig. 3C

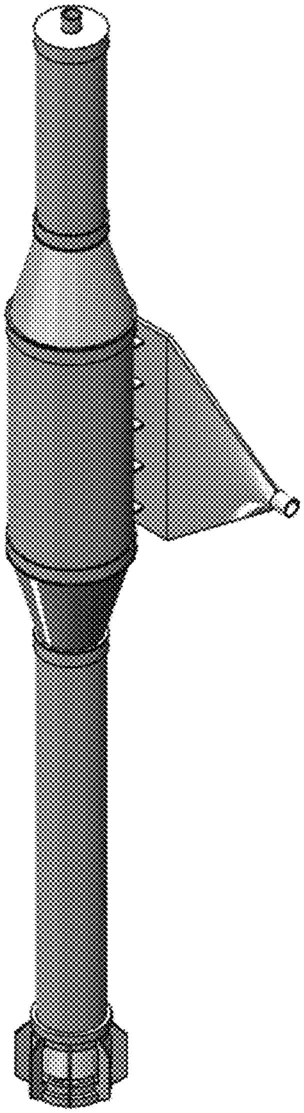

Fig. 4A

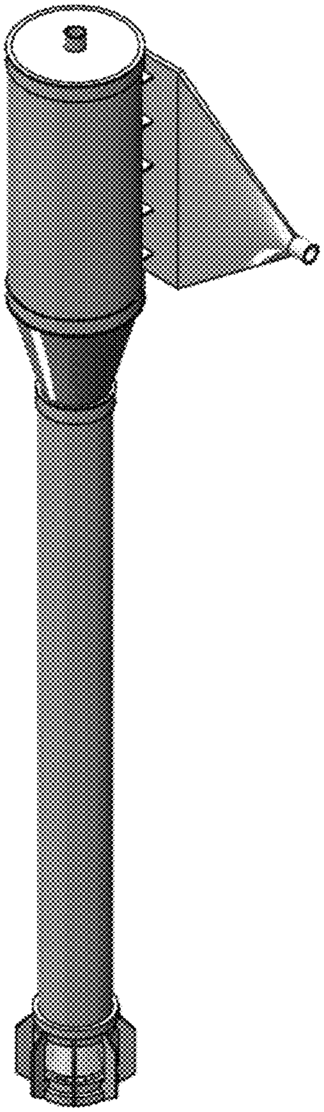

Fig. 4B

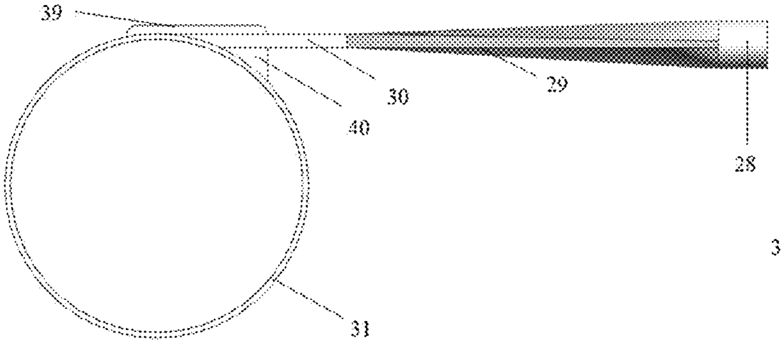

Fig. 5C

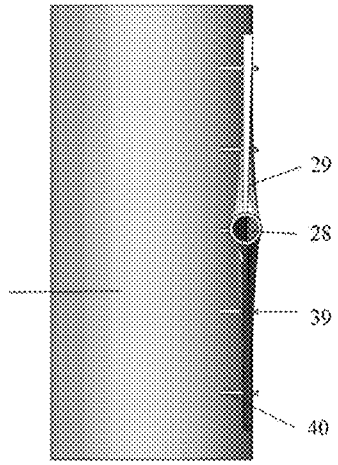

Fig. 5D

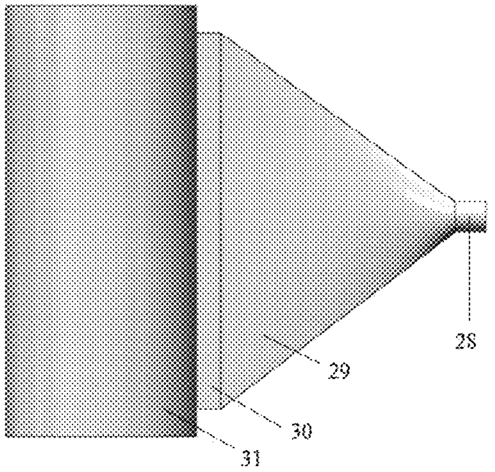

Fig. 5A

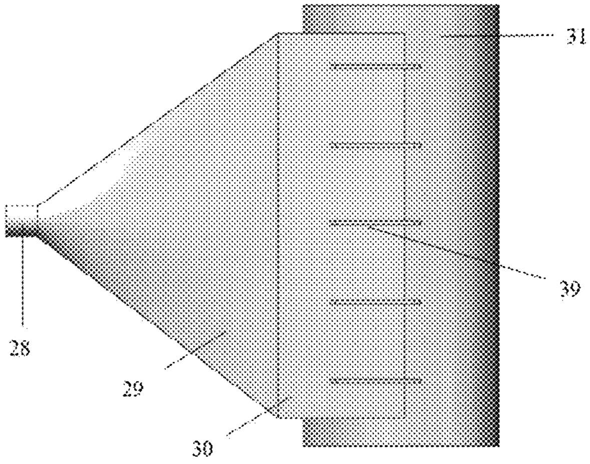

Fig. 5B

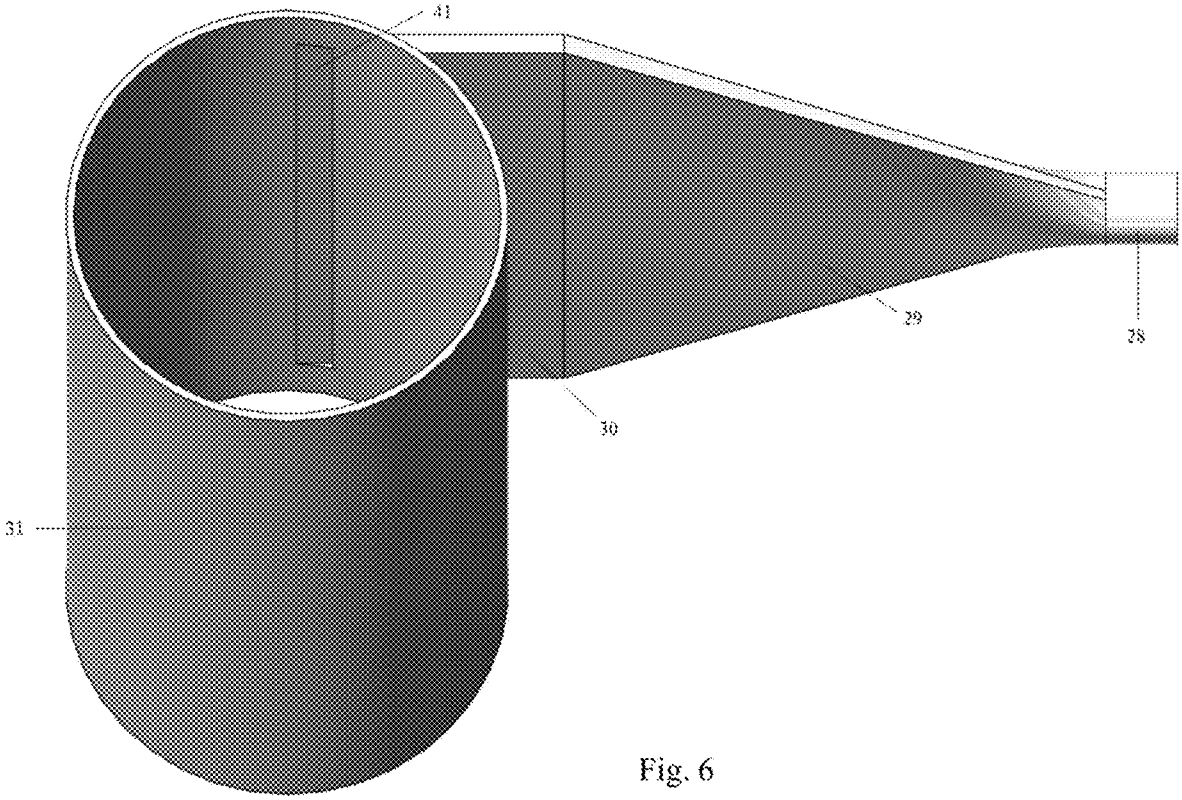

Fig. 6

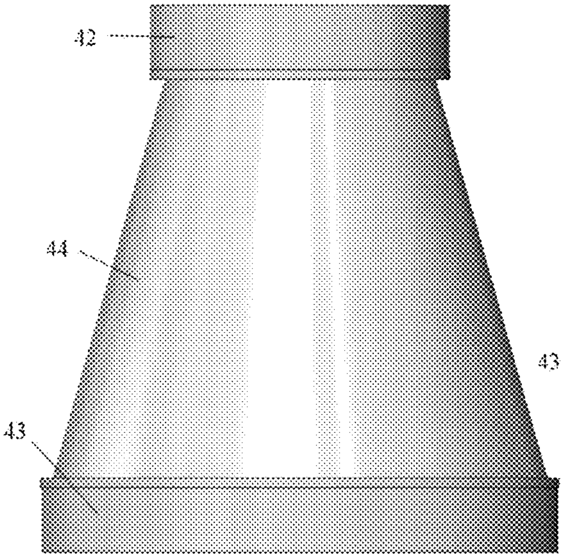

Fig. 7A

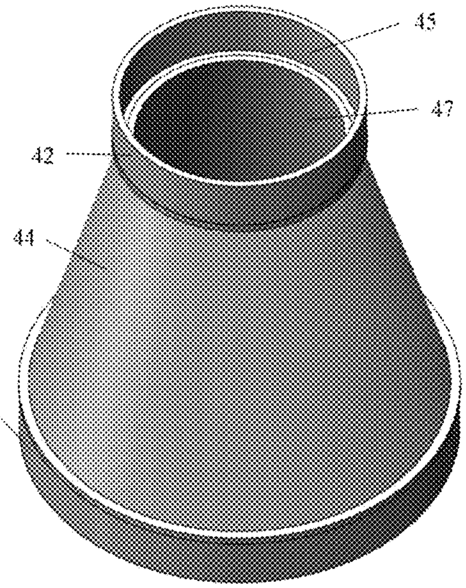

Fig. 7B

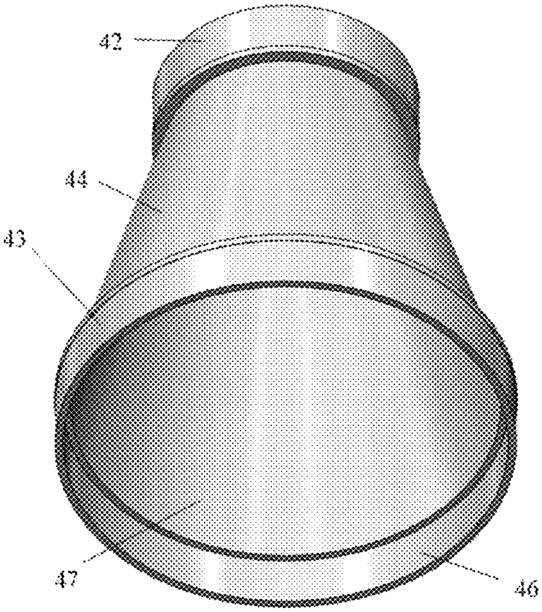

Fig. 7C

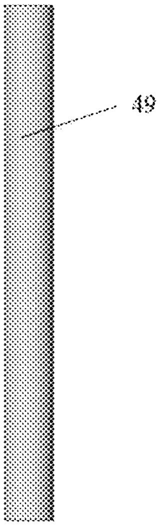

Fig. 8A

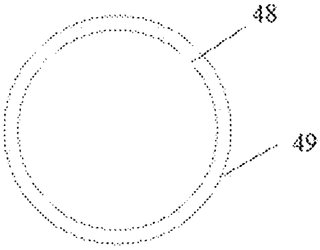

Fig. 8B

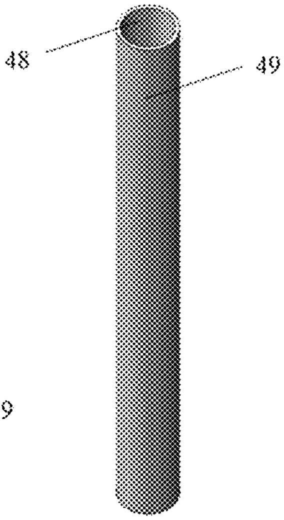

Fig. 8C

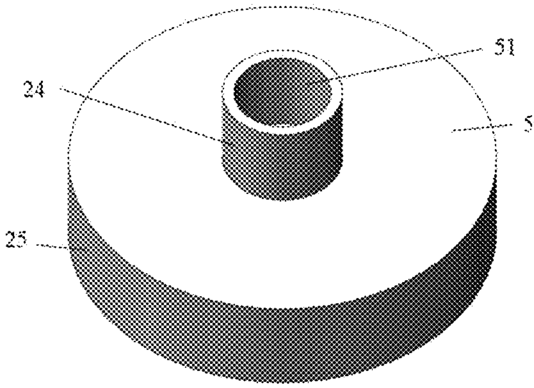

Fig. 9C

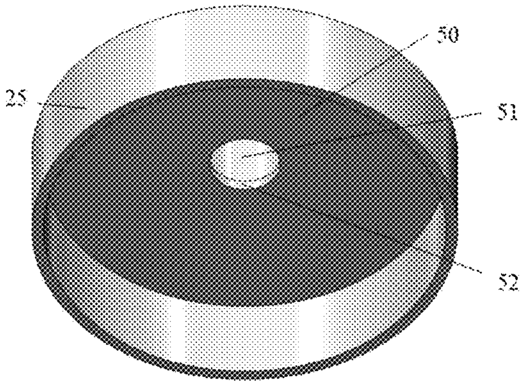

Fig. 9D

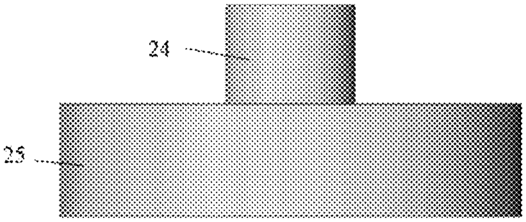

Fig. 9A

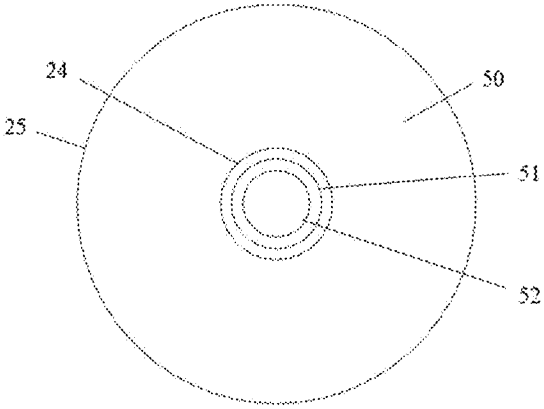

Fig. 9B

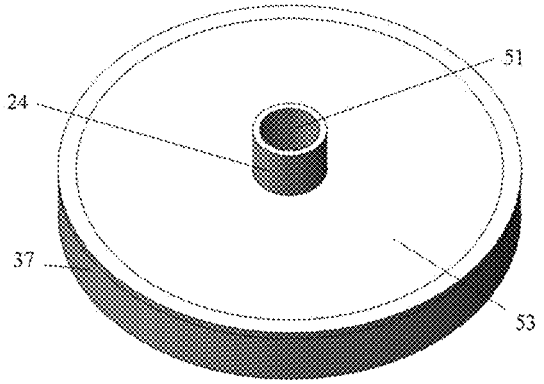

Fig. 10C

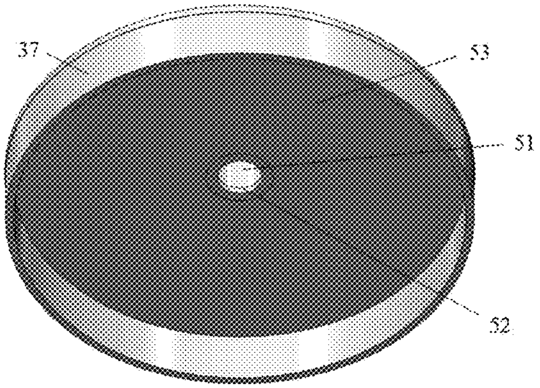

Fig. 10D

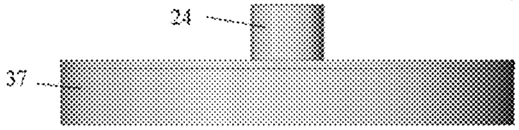

Fig. 10A

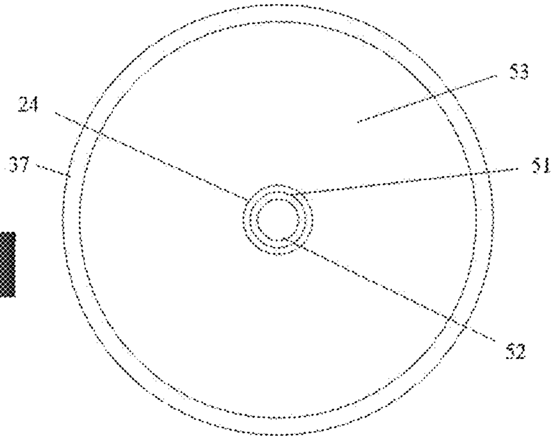

Fig. 10B

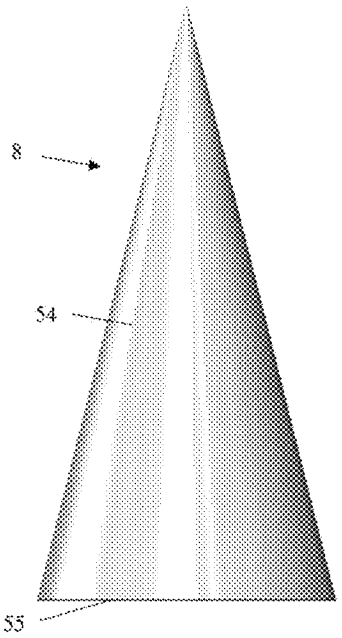

Fig. 11A

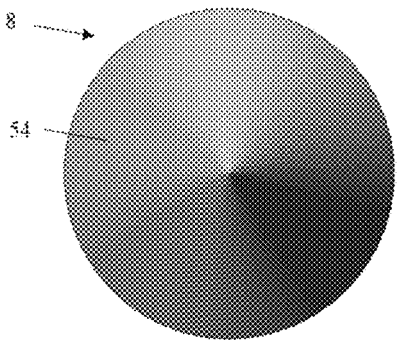

Fig. 11B

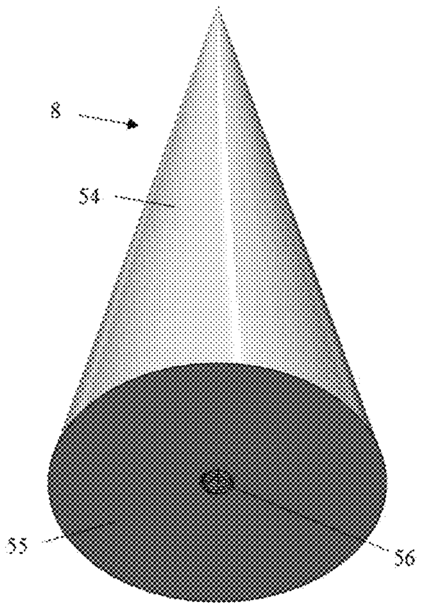

Fig. 11C

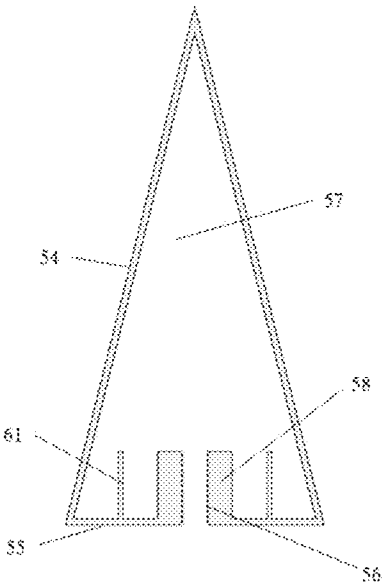

Fig. 12A

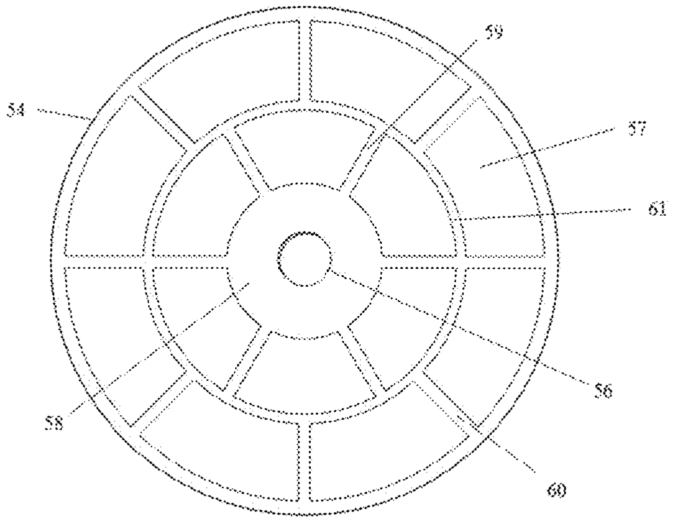

Fig. 12B

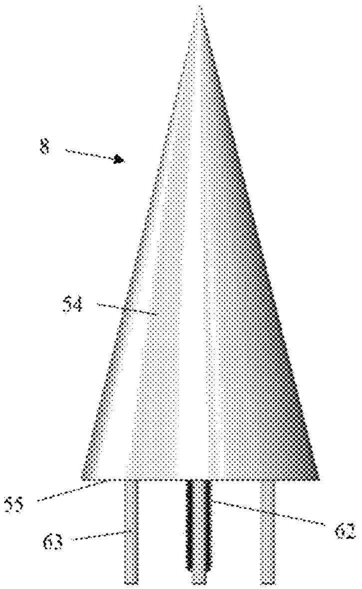

Fig. 13A

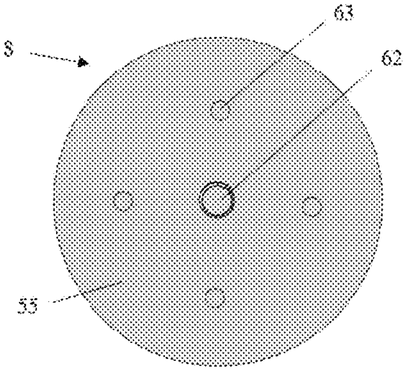

Fig. 13B

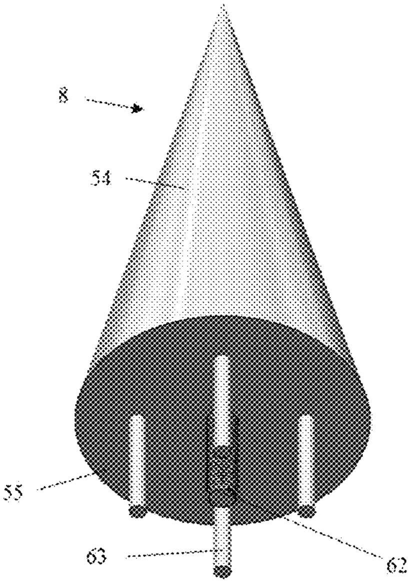

Fig. 13C

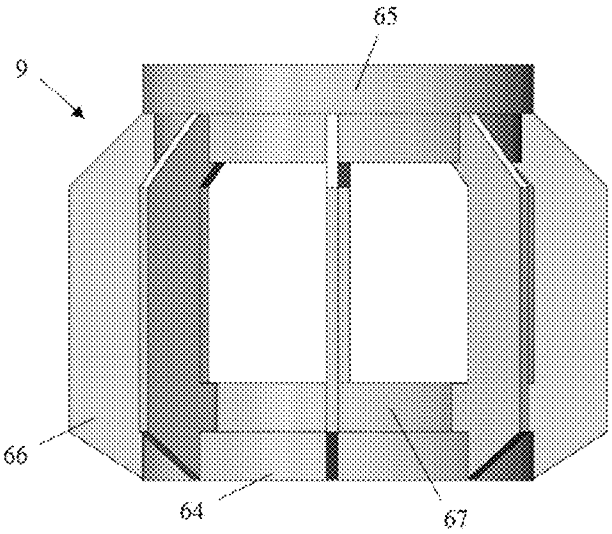

Fig. 14A

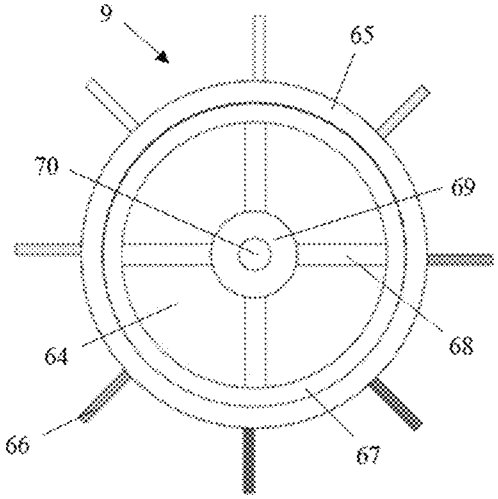

Fig. 14B

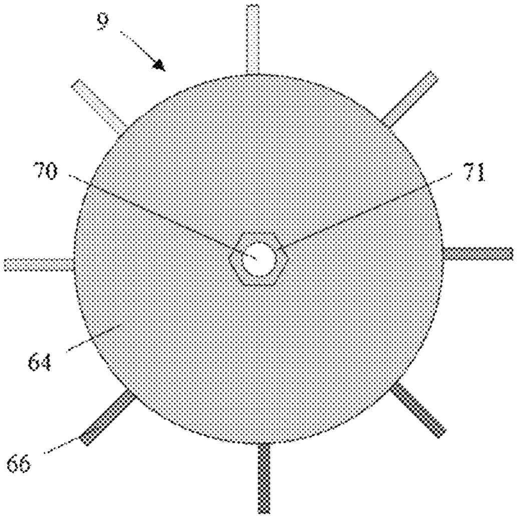

Fig. 14C

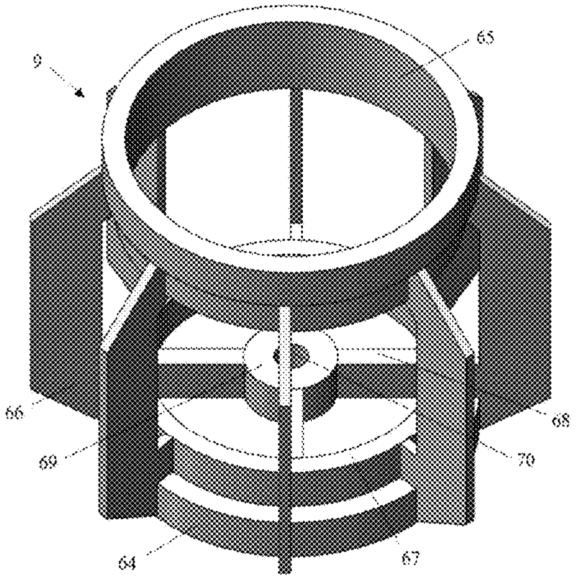

Fig. 15A

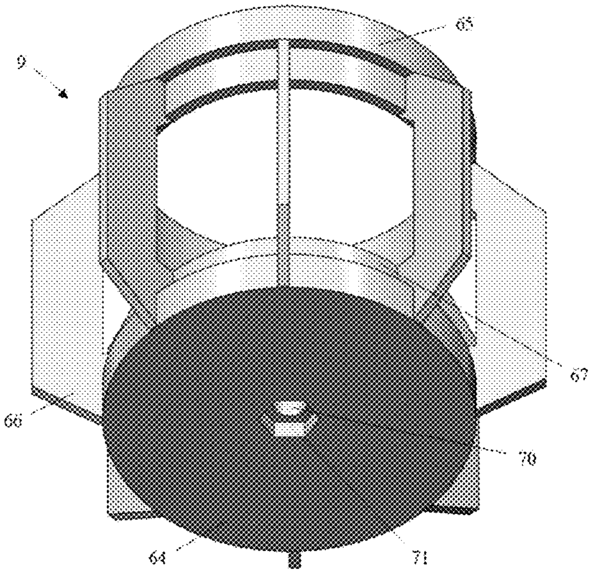

Fig. 15B

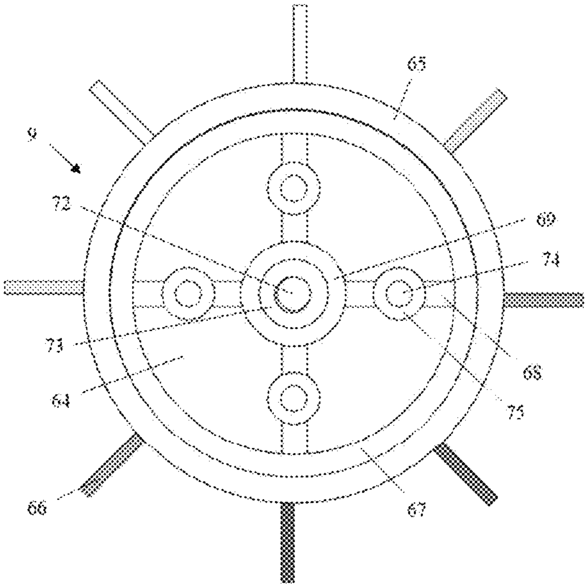

Fig. 16A

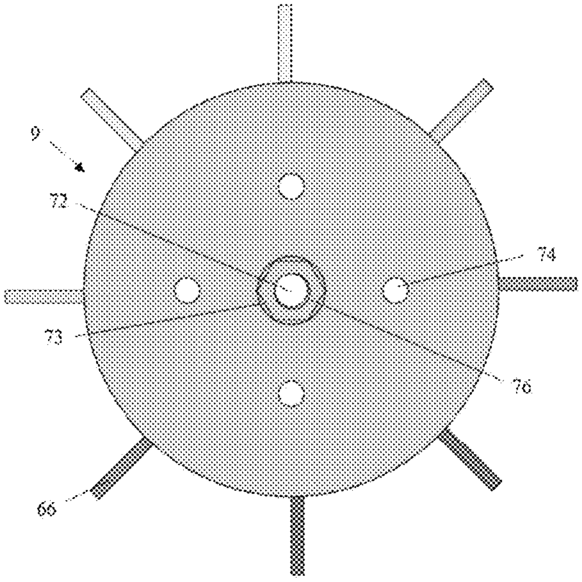

Fig. 16B

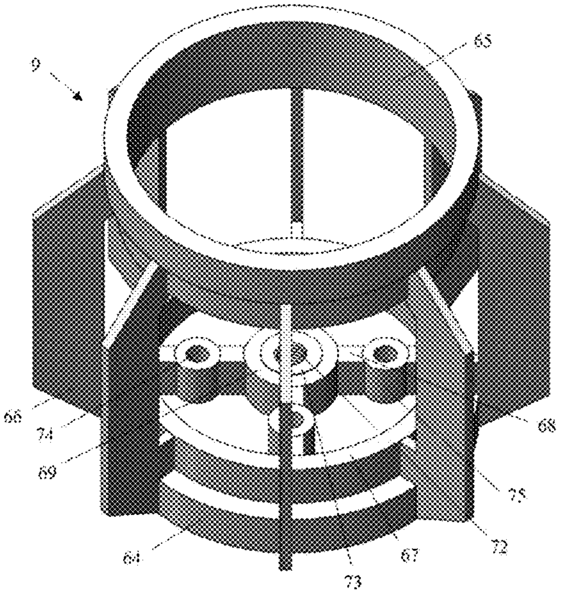

Fig. 17A

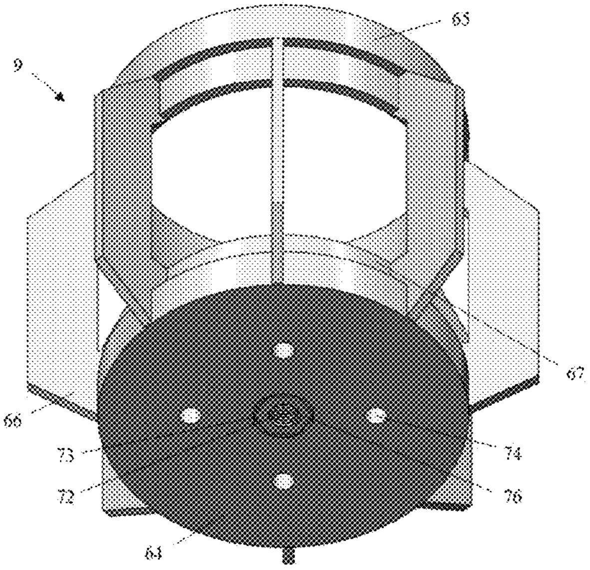

Fig. 17B

PROCESS AND APPARATUS TO REMOVE CARBON-14 FROM CARBON-DIOXIDE IN ATMOSPHERIC GASES AND AGRICULTURAL PRODUCTS GROWN IN CONTROLLED ENVIRONMENTS

CROSS REFERENCE TO RELATED APPLICATIONS

This application is a continuation of U.S. patent application Ser. No. 17/159,517 filed on Jan. 27, 2021, which is a divisional of U.S. patent application Ser. No. 16/030,734 filed on Jul. 9, 2018, which claims the benefit of U.S. Provisional Application Ser. No. 62/535,211, filed on Jul. 20, 2017. The complete disclosures of the above applications are hereby incorporated by reference for all purposes.

BACKGROUND

This invention relates to a process and apparatus for growing agricultural products with a reduced abundance of carbon-14 (^{14}C) by employing centrifugal separation of atmospheric gases to remove carbon dioxide (CO_2) with radioactive ^{14}C. Agricultural products with reduced ^{14}C content can be grown in controlled environments for the benefit of reducing harmful damage to human DNA that is unavoidable with our current food chain, due to the natural abundance of ^{14}C in atmospheric gases. Radioactive ^{14}C decay to nitrogen-14 with the release of 156 KeV has long been known to have biological effects (Purdom, C. E.). Sequencing of the human genome has identified 6.1 billion base pairs in human DNA, with 119 billion carbon atoms in the DNA of each nucleated cell (Lander, E. S., and Genome Reference Consortium (GRC) Human Genome Assembly build 38 (GRCh38)). Recent quantitative analysis of human tissues has estimated 3 trillion nucleated cells in the human body (Sender, R., Fuchs, S., & Milo, R.). Given the natural abundance and half-life of ^{14}C and composition of our genome (i.e., a mean of roughly 6.0×10^9 base pairs with 19.5 carbon atoms each), in the average human this decay is occurring once per second in human DNA, resulting in potential bond ruptures, DNA strand breakage, and nitrogen substitution in canonical bases (Sassi, M., et. al.). This cumulative damage has been positively correlated to cancer diagnoses (Patrick, A. D., & Patrick, B. E.), and may have other yet-to-be-quantified effects on human tissues as we age. In fact, no mammal has yet lived without this cumulative damage, so the qualitative benefits of precluding this genetic alteration are yet-to-be-quantified. To preclude this cumulative damage and genetic alteration, it is necessary to perform isotope separation on large volumes of atmospheric gases to remove ^{14}C from agricultural products and their derivatives in the food chain. This requires an economical means for the filtration of atmospheric gases and the growth of agricultural products in controlled environments.

BACKGROUND—PRIOR ART

In commercial applications, isotope separation has most commonly been applied to uranium isotopes utilizing a centrifugal separation process. The helikon vortex has been applied to uranium isotope enrichment in South Africa utilizing a multi-stage cascade design (Feiverson, H. A., Glaser, A., Mian, Z., & Von Hippel, F. N., and Moore, J. D. L.), but has not been applied to the selective isotope separation of CO_2 from atmospheric gases in prior art.

Turner, et al., in U.S. Pat. No. 8,460,434, shows that a helikon vortex can be utilized as a centrifugal separator in a multi-stage cascade design as one part of a process to separate methane from landfill gas. Although the multi-stage cascade design of the helikon vortex can separate gases by molecular density, it was developed for the separation of uranium isotopes, which are very heavy and differ in mass by a small amount (i.e., ^{235}U and ^{238}U, which differ in mass by 1.3%), which is one of the most challenging applications for centrifugal separation. Due to this multi-stage cascade design, it is very energy intensive to operate, and although it can be applied to the separation other gases by molecular density, it is uneconomical for the filtration of atmospheric gases on a large-scale for agricultural production.

Shacter, in U.S. Pat. No. 3,925,036, shows a method for cycling gases through a cascade of multiple stages to achieve the separation other gases by molecular density. This multi-stage cascade design was also intended for the separation of uranium isotopes, and due to the reasons noted above is very energy intensive to operate, and although it can be applied to the separation other gases by molecular density, it is uneconomical for the filtration of atmospheric gases on a large-scale for agricultural production.

Steimel, in U.S. Pat. No. 3,004,158, shows that a gas centrifuge can separate molecules of different masses by applying extremely high velocities while utilizing ionization of the gas with electric currents and the control of magnetic fields around the gas chamber. Although this process is effective for the separation of isotopes of heavy elements, such as uranium (i.e., ^{235}U and ^{238}U, which differ in mass by 1.3%), it is very energy intensive to operate and the apparatus itself is complex to construct, including a large electromagnet, electrodes, and controlling mechanisms. While all of this may be essential for the difficult and energy intensive separation of heavy isotopes from each other (e.g., ^{235}U and ^{238}U), the separation of carbon isotopes (e.g., ^{12}C and ^{14}C, which differ in mass by 16.7%) is much less energy intensive, due to the relatively large mass difference between isotopes. Being more energy intensive than necessary for the desired application, this process is uneconomical for the filtration of atmospheric gases on a large-scale for agricultural production.

Gerber, in U.S. Pat. No. 3,594,573, shows that heavy and light isotopes can be separated from a fluid by applying a rotating electric field and ionization of the liquid with electrodes or a radioactive source. Although this process may have economical applications for liquids at atmospheric pressures, utilization of this process for the separation of CO_2 with ^{14}C from atmospheric gases would first require the separation of CO_2 from other atmospheric gases, the liquification of the removed CO_2, and then the application of the described process. After this, the CO_2 without ^{14}C would need then to be re-combined with atmospheric gases without CO_2. Together, with the added complexity of removing CO_2 from atmospheric gases, liquification of this gas, application of the described process, and then recombination of gases, this approach is uneconomical for the filtration of atmospheric gases on a large-scale for agricultural production.

Janes, in U.S. Pat. No. 3,939,354, shows that ions can be separated from a plasma source utilizing mass acceleration. Similarly, Drummond, et al., in U.S. Pat. No. 3,942,975, shows that matter can be converted by an arc heater into an ionized plasma in excess of 5,000° K and stabilized with magnetic fields. Although this process was developed for the separation of rare valuable elements, such as metals, these could be adapted to separate carbon isotopes from sources of carbon. Utilization of these methodologies for the separation of CO_2 with ^{14}C from atmospheric gases would first require the separation of CO_2 from other atmospheric gases, then application of the described process to the removed CO_2 (or conversion of some other carbon source to plasma) and then removal of ^{14}C. After this, the carbon without ^{14}C would need to be combined with oxygen to produce CO_2, which would then need to be mixed with the atmospheric gases that had the CO_2 removed earlier. Together, with the added complexity of removing CO_2 from atmospheric gases, application of the described process, conversion of carbon to CO_2, and then recombination of gases, this appears to be an uneconomical alternative for the filtration of atmospheric gases on a large-scale for agricultural production. McKinney, et al., in U.S. Pat. No. 3,421,334, shows that isotopes of helium can be separated while in liquid form by exploiting unique physical properties of different isotopes. Although the claim was limited for use with helium, a similar approach could exploit the physical properties of CO_2 in a liquid state. This approach would be complicated by the fact CO_2 is a compound rather than an element and that there are three stable isotopes of oxygen (i.e., ^{16}O, ^{17}O, and ^{18}O) that are naturally found in combinations with three naturally occurring isotopes of carbon (i.e., ^{12}C, ^{13}C, and ^{14}C). Even so, exploiting the unique molecular weight of $^{12}C^{16}O_2$ in a liquid state would require the removal of all CO_2 from atmospheric gases, application of this new process, and then recombination of the CO_2 without ^{14}C with the atmospheric gases without CO_2. Altogether, even if this claim were modified for this application, it would also appear to be an uneconomical alternative for the filtration of atmospheric gases to remove ^{14}C on a large-scale for agricultural production.

Russ, Fischer, and Crawford, in U.S. Pat. No. 7,332,715 (2008), shows that gas at an atmospheric pressure can be passed through an ionization chamber with an electrode that generates ions, which pass through an ion filter apparatus with voltage differentials, thereby performing mass spectrometry, which demonstrates one form of isotope separation. Although this process is useful for the identification and measurement of the molecular and isotopic constituents of a gas, it is not readily extensible or adaptable to the removal of one isotopic component of atmospheric gases on a large scale, since each molecule of atmospheric gas needs to be ionized prior to filtration.

Lashoda, et al, in U.S. Pat. No. 4,584,073, shows that isotopes of an element in a compound can be separated utilizing a laser when the compound is deposited in a monolayer on small glass beads. Although this process has useful applications, utilization of this process for separation of CO_2 with ^{14}C from atmospheric gases would first require the separation of CO_2 from all other atmospheric gases, the liquification of the removed CO_2, and then the application of the described process. After this, the CO_2 without ^{14}C would then need to be re-combined with atmospheric gases without CO_2. Together, with the added complexity of removing CO_2 from atmospheric gases, liquification of the removed CO_2 gas, application of the described process, and then recombination of gases, this approach is uneconomical for the filtration of atmospheric gases on a large-scale for agricultural production.

Several instances of prior art utilize condensation of gases or condensates as part of a system or method to remove isotopes. Redmann, in U.S. Pat. No. 4,638,674, shows that isotopes can be removed from a continuous stream of gas through condensation, although the claims are limited to gas streams from a nuclear plant rather than atmospheric gases. Similarly, Schweiger in U.S. Pat. No. 4,816,209, shows that radioactive tritium isotopes can be removed from gas from a nuclear reactor by utilizing condensation. These claims are also limited to gases from nuclear reactors.

Janner, et al., in U.S. Pat. No. 4,311,674, shows that one isotope component of gases can be selectively excited from a condensate using radiation from a laser. Utilization of this process for separation of CO_2 with ^{14}C from atmospheric gases would first require the condensation of CO_2 from all other atmospheric gases by increasing the pressure of the gases to exceed 5.1 bars, and then application of the described process. After this, the CO_2 without ^{14}C would then need to be re-combined with atmospheric gases without CO_2. Together, with the added complexity of removing CO_2 from atmospheric gases, liquification of the removed CO_2 gas, application of the described process, and then recombination of gases, this approach is uneconomical for the filtration of atmospheric gases on a large-scale for agricultural production.

Wikdahl, in U.S. Pat. No. 4,070,171, shows that gas mixtures can be separated by molecular or atomic weight by centrifugal force in a vortex. The described apparatus utilizes velocities exceeding the speed of sound and has been utilized for uranium isotope separation, which is among the most technically difficult isotope separation applications. This apparatus could be adapted for the less rigorous application of ^{14}C separation, although the small diameter limits the utility for the filtration of atmospheric gases on a large-scale for agricultural production, and effective ^{14}C separation can be achieved at lower velocities than those required for more demanding applications. Therefore, this apparatus would be less economical than an alternative that does not require such extremely high velocities, which limits efficiency, and such a small diameter, which limits the volume of throughput.

Mangadoddy, et al., in U.S. Pat. No. 9,579,666 B2, shows that dense medium can be separated by centrifugal force in a vortex. Although this apparatus appears very similar to Wikdahl's apparatus, as noted above, it has a larger diameter, is intended for the separation of particles rather than molecules, and is functional at lower velocities. Although this apparatus was not intended for isotope separation, and that subject is outside the scope of the claims, it could be modified and adapted for the application of separating CO_2 with ^{14}C from atmospheric gases. In conclusion, no method or process has been formerly developed for maintaining a controlled environment from which CO_2 with ^{14}C has either been removed or reduced to a lower level than the natural abundance of ^{14}C, as required for growing agricultural products with reduced ^{14}C content. Similarly, no apparatus has been formerly developed with the specific intent to efficiently and economically remove CO_2 with ^{14}C from atmospheric gases with a single filtration pass, as required for large scale agricultural production.

SUMMARY

A process to grow agricultural products with a reduced abundance of radioactive ^{14}C will have health benefits by reducing harmful damage to human DNA, which has been correlated to cancer. Other benefits of reduced cumulative genetic damage over long periods of time have yet to be quantified. To-date, removal of ^{14}C from agricultural products on a large scale has not been possible due to a lack of an economical means to remove ^{14}C from CO_2 on a scale sufficient for agricultural production. Such agricultural products can be grown in a large variety of controlled environments so long as they are airtight, such as a sealed container,

greenhouse, or building, and provided the other requirements for agricultural growth are also satisfied, such as light, water, and micronutrients. The controlled environment must be airtight so that the gases therein can be controlled and constitute filtered atmospheric gases from which CO_2 with ^{14}C has been removed. With the proper sensors, control valves, and control systems, 1) the abundance of CO_2 in the controlled environment can be automatically maintained by circulating atmospheric gases through the filtration system, operating control valves, and circulation of fresh filtered air through the controlled environment, 2) to ensure the quality of the agricultural products, the control system can also ensure the filtration system is effective prior to routing filtered atmospheric gases into the controlled environment, and 3) the air pressure inside the controlled environment can be maintained at a positive pressure with respect to the external atmospheric air pressure, to prevent any leakage that could contaminate the controlled environment. Together with hydroponic growing methodologies, this process enables the complete automation of large scale agricultural production with reduced ^{14}C.

The bilateral and unilateral compression helikon vortex designs provide efficient, single-pass systems for the effective filtration of ^{14}C from CO_2 that is suitable for the filtration of large quantities of atmospheric gases as required for agricultural production (Patrick, A. D., & Patrick, B. E.). These designs are effective due to the relatively large mass difference between stable carbon and unstable carbon isotopes (i.e., ^{12}C and ^{14}C, which differ in mass by 16.7%), which is much less energy intensive to separate than the typical subjects of nuclear isotope separation, i.e., the heavy element isotopes of uranium, such as ^{235}U and ^{238}U, which differ in mass by 1.3% and require much more energy to separate. The designs also benefit from the fact unlike uranium, which is a scarce resource and cannot be wasted, atmospheric gases are relatively abundant and available for filtration at no material cost. Therefore, if a portion of perfectly usable air is lost as "waste" from the filtration process, there is no material cost for the separation process, and consequently, the filtration process does not require a high level of material efficiency to be successful or effective at removing ^{14}C. The designs are simple without requiring electromagnets or electrodes for the ionization of gas, like some isotope separation methodologies. Also, many of the designs that utilize or require the ionization of gas are more complex and resource intensive to construct and operate. The single-pass system designs are also efficient without requiring a multi-stage cascade design, which requires many more resources to build than a single-pass filtration system, as well as much more energy to operate. The designs are more efficient in both design and operation than any of the designs that require liquification of the gases, or ionization of liquified gases, which introduce the process complexities of liquifying atmospheric gases, the maintenance hazards of operating with highly pressurized systems, and the recombination of filtered gases after liquification. The designs are also more efficient and economical than processes that would require converting CO_2 to plasma and stabilizing ionized plasma with magnetic fields. Since the designs only require the acceleration of atmospheric gases, they are also more efficient than processes that require ionization and processing of each molecule of gas in mixtures of gases being separated. Since the designs utilize atmospheric gases directly, they do not require condensation of gases from nuclear power plants or require the excitation of condensates by lasers, which would only add inefficiencies. The designs do not require the acceleration of gases to velocities exceeding the speed of sound, which is required for centrifugal gas separation methodologies applied to more technically difficult isotope separation applications. The designs also do not require the very small diameter of apparatus required by centrifugal gas separation systems intended for more technically challenging isotope separation applications. Since the designs are effective at lower velocities and larger diameters, they are more efficient and well suited for the high throughput of atmospheric gases volumes required for large scale agricultural production applications. The designs are not constrained by particulate separation, only the densities of atmospheric gases, and any particulates that enter the designs would generally be discarded with the high-density atmospheric gases, including the CO_2 with ^{14}C. The designs are intended to efficiently and economically remove CO_2 with ^{14}C from atmospheric gases with a single-pass filtration, as required for large scale agricultural production.

DRAWINGS—FIGURES

FIG. **1** is a Flow Diagram for the Separation of Atmospheric Gases to Remove CO_2 with ^{14}C Utilizing a Helikon Vortex and Control System.

FIGS. **2**A to **2**D are various views of a Bilateral Compression Helikon Vortex Overview.

FIGS. **3**A to **3**D are various views of a Unilateral Compression Helikon Vortex Overview.

FIGS. **4**A and **4**B are Perspective Views of a Bilateral Compression Helikon Vortex (FIG. **4**A) and a Unilateral Compression Helikon Vortex (FIG. **4**B).

FIGS. **5**A to **5**D are various views of a Wide Vortex Chamber with Tangential Input Overview.

FIG. **6** is a Perspective View of a Wide Vortex Chamber with Tangential Input.

FIGS. **7**A to **7**C are various views of a Lateral Vortex Chamber Adapter Overview.

FIGS. **8**A to **8**C are various views of a Narrow Vortex Chamber Overview.

FIGS. **9**A to **9**D are various views of a Narrow Vortex Chamber Cap/Outlet Overview.

FIGS. **10**A to **10**D are various views of a Wide Vortex Chamber Cap/Outlet Overview.

FIGS. **11**A to **11**C are various views of a Manually Calibrated Helikon Vortex Cone Overview.

FIGS. **12**A and **12**B are various cross-section views of a Manually Calibrated Helikon Vortex Cone.

FIGS. **13**A to **13**C are various views of an Alternative Threaded Cone Overview.

FIGS. **14**A to **14**C are various views of a Vortex Exhaust/Cone Alignment Base Overview.

FIGS. **15**A and **15**B are various perspective views of a Vortex Exhaust/Cone Alignment Base.

FIGS. **16**A and **16**B are various views of a Vortex Exhaust/Alternative Threaded Cone Alignment Base Overview.

FIGS. **17**A and **17**B are various perspective views of a Vortex Exhaust/Alternative Threaded Cone Alignment Base.

DETAILED DESCRIPTION

FIG. **1**. is a flow diagram for the separation of atmospheric gases to remove CO_2 with ^{14}C in accordance with the process, control system, and Helikon Vortex Bilateral and Unilateral Compression designs within the invention. The Helikon Vortex **1** (see FIGS. **2**A-**2**D or FIGS. **3**A-**3**D for details) constitutes a means to remove CO_2 with ^{14}C from the atmospheric gases **2**. Several alternative processes or apparatus could substitute **1** in this flow diagram, with respective losses of efficiency as described in the background section, and constitute an alternative means to remove CO_2 with ^{14}C from **2**. The atmospheric pressure p_1 of the atmospheric gases **2** is measured by pressure sensor **3** and CO_2 abundance c_1 in the atmospheric gases **2** is measured by CO_2 sensor **4**, both of which are monitored by a control system **13**. A commercial high-speed air blower **5**, which can be activated by the control system **13**, accelerates the atmospheric gases to velocity v and volume V_0 per second which is output directly into an airflow adapter **6** which is connected to the vortex chamber **7**, into which the air is injected tangentially to maximize centrifugal acceleration. A cone **8** which is aligned with the vortex chamber **7** by the vortex exhaust/cone alignment base **9**. The position of the cone **8** can be raised or lowered relative to the vortex chamber **7** to reduce or widen the gap between the vortex chamber **7** and the cone **8**. The positioning of the cone **8** to achieve the desired separation is hereafter referred to as calibration. Dense molecular gas **10** is forced to the outside of the vortex chamber **7** by centrifugal acceleration a and exits the vortex chamber **7** through the gap near the cone **8**, where it is exhausted to the atmosphere, reentering the atmospheric gases **2**. Low density molecular gas **11** with reduced ^{14}C content is slowed by the cone **8** and exits the vortex chamber opposite the cone at the top. The calibration (or cone position) can be adjusted by an electrical motor **12** which can raise or lower the cone **8** position relative to the vortex chamber **7** through axial rotation. Low density molecular gas **11** can exit through either manual or solenoid operated electrical control valves **14** and **17**, which can be controlled by the control system **13**. Control valve **14** is a relief valve which opens and releases gases while the high-speed blower **5** is starting, while the vortex chamber is pressurizing, or while the cone position is changing during calibration. CO_2 abundance c_2 of the relief valve gas output **15** is measured at CO_2 sensor **16** and monitored by the control system **13**. Once the vortex chamber **7** is pressurized and CO_2 separation is adequate per the helikon vortex calibration, relief control valve **14** is closed and the vortex chamber control valve **17** is simultaneously opened by the control system **13**. CO_2 separation is adequate when CO_2 sensor calibration adjusted measurements $c_2/c_1<S$, where the required separation $S<1$, and S is dependent on the efficiency of the helikon vortex. While the vortex chamber control valve **17** (i.e., the control valve for gaseous input to the controlled environment) is open, the CO_2 abundance c_3 of the vortex chamber control valve output **18** is monitored by CO_2 sensor **19** to ensure CO_2 separation is adequate, per the helikon vortex calibration, and proper operation of the vortex. CO_2 separation is adequate when CO_2 sensor calibration adjusted measurements $c_3/c_1<S$. The vortex chamber control valve output **18** passes directly into a controlled environment **20** which can be used for applications requiring CO_2 with reduced ^{14}C content (e.g., agricultural production applications). The pressure p_2 of gases inside the controlled environment **20** is measured by a pressure sensor **21** and monitored by the control system **13** with to ensure a positive pressure (i.e., $p_2>p_1$) is maintained inside the controlled environment **20** to preclude contamination with CO_2 containing ^{14}C in the event of a leak or rupture. Control valve **22** remains closed while $p_2<p_1$ when **17** is open until **20** has a positive pressure differential over the atmospheric pressure (as determined by comparing pressure sensors **3** and **21**), or $p_2>p_1+p_0$, where p_0 is the minimum additional pressure required by **20**, to ensure atmospheric gases **2** do not enter **20** through **22**. When control valve **17** is open and a sufficient positive pressure exists in the controlled environment **20**, or $p_2>p_1+p_0$, control valve **22** will be opened by the control system **13**, allowing controlled environment gases **23** to exit through **22**, where it is exhausted to the atmosphere, reentering atmospheric gases **2**. Control valve **22** may also be opened by **13** when atmospheric pressure p_1 decreases so that $p_2>p_1+2*p_0$, as an emergency relief, to ensure the pressure in **20** is not so high that controlled environment gases **23** do not enter **7** through **17** when **17** is opened. When p_1 is rising, **13** can also turn on **5** to increase p_2 to maintain a positive pressure in **20**; as described above, **5** pressurizes **7**, whereby **17** is opened, increasing p_2. When CO_2 abundance decreases in **20** due to utilization or consumption by applications, as measured by c_3, and $c_3<c_0$, where c_0 is the minimum CO_2 abundance required by **20**, **13** will turn on **5** to replace the controlled environment gases in **20**. In this manner, **13** can regulate both the pressure and CO_2 abundance in the controlled environment **20** as the natural atmospheric pressure p_1 of 2 fluctuates and CO_2 with reduced ^{14}C content is utilized in **20**. The control system **13** can either be programmed or configured to operate **5**, **14**, **17**, and **22** utilizing electronic controls or switches with digital or analog signals, constituting a means to operate the blower and control valves. Similarly, **13** can either be programmed or configured to monitor digital or analog signals from **3**, **4**, **16**, **19**, and **21**, constituting a means to monitor the sensors.

FIGS. **2**A-**2**D are various views of a Bilateral Compression Helikon Vortex Overview, with a front view (FIG. **2**A), top view (FIG. **2**B), and right-side view (FIG. **2**C), and cross-section of the tangential airflow stabilizer (FIG. **2**D). This assembly is one instantiation of the helikon vortex **1** in FIG. **1**, and several components from FIG. **1** are recognizable here, including the airflow adapter **6**, helikon vortex chamber **7**, cone **8**, and helikon vortex exhaust/cone alignment base **9**. The vortex output adapter **24** is where CO_2 with reduced ^{14}C content is output, and this is attached to the narrow vortex chamber cap/outlet **25**, which is on top of **7**. The vortex chamber consists of the upper narrow vortex chamber **26**, extends through the center of the upper lateral vortex chamber adapter **27**, the center of the airflow adapter **6**, the center of the lower lateral vortex chamber adapter **32**, and the lower narrow vortex chamber **33**. The upper and lower narrow vortex chambers have an interior radius of r_1 and combined height of h_1, where the height of **26** is less than or equal to half the height of **33**. The airflow adapter **6** consists of several components identifiable here, including the blower input connector **28**, radial to tangential airflow adapter **29**, tangential airflow stabilizer **30**, and the wide vortex chamber with tangential input **31**. The wide vortex chamber has an interior radius of r_2 and height of h_2, and is connected to the narrow vortex chambers **26** and **33** of interior radius r_1 by **27** and **32**, each with a height h_3. The blower input connector **28** is a circular adapter with an interior radius of r_0 and thickness of t_0 for an exterior radius of r_0+t_0, providing a cross-section area of πr_0^2 for V_0 per second of input from the high-speed blower **5**. The radial to tangential airflow adapter **29** changes the radial airflow at **28** to a vertical stream at the tangential airflow stabilizer **30** with an interior stream height of h_0, a maximum width of w_0 where $\pi r_0^2 \geq h_0 w_0$. The stream cross-section **34** can be compressed to increase pressure in the vortex chamber or to achieve a higher input velocity based on the performance of **5**. The stream can also be tapered or shaped at the top and bottom excluding wedges from the tangential airflow **35** of height h_4 and width w_1 from the tangential edge closest to the center of the vortex chamber (See FIG. **2**D), where $h_4 \leq h_0/2$ and $w_1<w_0$, yielding a cross section area of h_0w_0-

$h_4w_1 \leq \pi r_0^2$, to evenly distribute pressure in **31** as gases are compressed in **27** and **32**. Below the vortex chamber **7**, the cone **8** is held in a position aligned with the center of **7** by the helikon vortex exhaust/cone alignment base **9** which is attached to the bottom of **33**. The position of **8** can be adjusted for calibration of the helikon vortex while remaining in alignment with the lower narrow vortex chamber **33**. The top view (FIG. **2**C) obstructs components below **31**, but shows reinforcement for the tangential airflow **36**, which is also visible on the right-side view (FIG. **2**C).

The interior volume of the Bilateral Compression Helikon Vortex as defined is

$$V=\pi r_1^2h_1+\pi r_2^2h_2+2\pi(r_1^2+r_1r_2+r_2^2)h_3/3.$$

FIGS. **3**A-**3**D are various views of a Unilateral Compression Helikon Vortex Overview, with a front view (FIG. **3**A), top view (FIG. **3**B), and right-side view (FIG. **3**C), and cross-section of the tangential airflow stabilizer (FIG. **3**D). This assembly is one instantiation of the helikon vortex **1** in FIG. **1**, and several components from FIG. **1** are recognizable here, including the airflow adapter **6**, helikon vortex chamber **7**, cone **8**, and helikon vortex exhaust/cone alignment base **9**. The vortex output adapter **24** is where CO_2 with reduced ^{14}C content is output, and this is attached to the wide vortex chamber cap/outlet **37**, which is on top of 6. The vortex chamber consists of the lower narrow vortex chamber **33**, and extends through the lower lateral vortex chamber adapter **32**, and the center of the airflow adapter **6**. The lower narrow vortex chamber has an interior radius of r_1 and height of h_1. The airflow adapter **6** consists of several components that are identifiable here, including the blower input connector **28**, radial to tangential airflow adapter **29**, tangential airflow stabilizer **30**, and the wide vortex chamber with tangential input **31**. The wide vortex chamber has an interior radius of r_2 and height of h_2, and is connected to the narrow vortex chamber **33** of interior radius r_1 by **32**, with a height h_3. The blower input connector **28** is a circular adapter with an interior radius of r_0 and thickness of t_0 for an exterior radius of r_0+t_0, providing a cross-section area of r_0^2 for V_0 per second of input from the high-speed blower **5**. The radial to tangential airflow adapter **29** changes the radial airflow at **28** to a vertical stream at the tangential airflow stabilizer **30** with an interior stream height of h_0, a maximum width of w_0 where $\pi r_0^2 \geq h_0w_0$. The stream cross-section **34** can be compressed to increase pressure in the vortex chamber or to achieve a higher input velocity based on the performance of **5**. The stream can also be tapered or shaped at the bottom excluding a wedge from the tangential airflow **35** of height h_4 and width w_1 from the tangential edge closest to the center of the vortex chamber (See FIG. **3***d*), where $h_4 \leq h_0/2$ and $w_1 < w_0$, yielding a cross section area of $h_0w_0-h_4w_1/2 \leq \pi r_0^2$, to evenly distribute pressure in **31** as gases are compressed in **32**. Below the vortex chamber **7**, the cone **8** is held in a position aligned with the center of **7** by the helikon vortex exhaust/cone alignment base **9** which is attached to the bottom of **33**. The position of **8** can be adjusted for calibration of the helikon vortex while remaining in alignment with the lower narrow vortex chamber **33**. The top view (FIG. **3**B) obstructs components below **31**, but shows reinforcement for the tangential airflow **36**, which is also visible on the right-side view (FIG. **3**C).

The interior volume of the Unilateral Compression Helikon Vortex as defined is

$$V=\pi r_1^2h_1+\pi r_2^2h_2+\pi(r_1^2+r_1r_2+r_2^2)h_3/3.$$

FIGS. **4**A-**4**D are Perspective Views of a Bilateral Compression Helikon Vortex (FIG. **4**A) and a Unilateral Compression Helikon Vortex (FIG. **4**B).

FIGS. **5**A-**5**D are various views of a Wide Vortex Chamber with Tangential Input Overview, with a front view (FIG. **5**A), back view (FIG. **5**B), top view (FIG. **5**C), and right-side view (FIG. **5**D). On all four views, the blower input connector **28**, the radial to tangential airflow adapter **29**, and the wide vortex chamber with tangential input **31** are visible. On all but the right-side view, the tangential airflow stabilizer **30** is visible. Cross-sections of **30** are provided in FIGS. **2**D and **3**D, detailing the interior cross-section area of the tangential airflow stabilizer **34** and variable exclusion wedges **35** detailed above, as related to the radius r_0 of **28**. The outer reinforcement for the tangential airflow **39** are clearly seen on FIG. **5**B, FIG. **5**C, and FIG. **5**D. These are evenly spaced vertically and centered around the input axis of **28**, providing reinforcement for both **30** and **31** near the tangential input. The inner reinforcement for the tangential airflow **40** are seen on FIG. **5**C and FIG. **5**D, and are also evenly spaced vertically and centered around the input axis of **28**, providing reinforcement for both **30** and **31** near the tangential input.

FIG. **6** is a Perspective View of a Wide Vortex Chamber with Tangential Input. From this front-upper perspective view the tangential airflow vent **41** is visible inside **31**, which was not visible from any of the four views on FIGS. **5**A-**5**D. As illustrated in FIG. **6**, **41** has tangential dimensions with a height of h_0 and width of w_0 and is configured for either a bilateral or unilateral helikon vortex configuration with $h_4=0$ and $w_1=0$, omitting any exclusion wedges (i.e., **35**) from the tangential airflow. The airflow adapter **6**, as seen on FIGS. **1**, **2**, and **3**, utilizes **28**, **29**, **30**, and **35**, as seen on FIGS. **2**A-**2**D and **3**A-**3**D, to constitute a means to stabilize and shape the airflow of said atmospheric gases **2** into **34**, as seen on FIGS. **2**A-**2**D and **3**A-**3**D, prior to passing through **41** into **31**, as seen here on FIG. **6**.

FIGS. **7**A-**7**C are various views of a Lateral Vortex Chamber Adapter Overview, with a front view (FIG. **7**A), upper-front perspective view (FIG. **7**B), and lower-front perspective view (FIG. **7**C). The lateral vortex chamber adapter is utilized twice in the bilateral compression helikon vortex configuration **27** and **32**, and once in the unilateral compression helikon vortex configuration **32**. The lateral adapter **44** connects to a wide vortex chamber **32** with a wide vortex chamber connector **42** and connects to a narrow vortex chamber to a narrow vortex chamber **26** or **33** with a narrow vortex chamber connector **43**. As illustrated in FIG. **7**B, the interior of the narrow vortex chamber connector **45** has a radius equal to the outside radius of the narrow vortex chamber (See FIGS. **8**A-**8**C). The interior of the lateral adapter **47** is a smooth surface in the shape of a truncated cone and has a radius of r_1 at the minimum radius at the edge shared with **45**. The interior of the wide vortex chamber connector **46** has a radius equal to the outside radius of the wide vortex chamber **31**. The maximum radius of **47** is equal to r_2 at the edge shared with **46**. Thereby, **47** provides a smooth surface inside the vortex chamber of height h_3 between **45** and **46** for the compression of gases for separation by centrifugal acceleration while connecting wide and narrow vortex chamber components.

FIGS. **8**A-**8**C are various views of a Narrow Vortex Chamber Overview, with a front view (FIG. **8**A), top view (FIG. **8**B), and upper-front perspective view (FIG. **8**C). The narrow vortex chamber is utilized twice in the bilateral compression helikon vortex configuration **26** and **33**, and once in the unilateral compression helikon vortex configuration **33**. To reduce helikon vortex manufacturing costs, commercial pipe with standard inner and outer diameters can be utilized for narrow vortex chambers by sizing the connectors on all connecting components, including **9**, **25**, **27**, and **32**, to match the outer and inner diameters of standard commercial pipe(s). For instance, the interior diameter of narrow vortex chamber connector **45** must match the outer diameter of the exterior of the narrow vortex chamber **49**, and the minimum interior diameter of **47** must match the interior diameter of **48**. An example of adapting a commercial pipe would be a 3 inch Schedule 40 PVC pipe, in which case the outer diameter of **49** would be 88.9 mm and the interior diameter of **48** would be 76.2 mm. Any commercial pipes must be cleaned with solvents and in the case of plastic or related synthetic polymers (e.g., polyvinyl chloride), they must be rigid and the interior of the narrow vortex chamber **48** must be coated with an antistatic treatment prior to utilization.

FIGS. **9**A-**9**B are various views of a Narrow Vortex Chamber Cap/Outlet Overview, with a front view (FIG. **9**A), top view (FIG. **9**B), top upper-front perspective view (FIG. **9**C), and lower-front perspective view (FIG. **9**D). The narrow vortex chamber cap/outlet **25** is utilized in the bilateral compression helikon vortex, and the vortex output adapter **24** is visible in FIG. **9**A, FIG. **9**B, and FIG. **9**C. The top of the narrow vortex chamber cap **50** is visible on FIG. **9**B and FIG. **9**C. To reduce helikon vortex manufacturing costs, the interior dimensions of the vortex output adapter **24** are intended to connect to commercial pipe with standard inner and outer diameters. The interior of vortex output adapter **51**, visible in FIG. **9**B, FIG. **9**C, and FIG. **9**D, has a diameter matching the outer diameter of a commercial pipe, while the vortex chamber cap outlet **52**, visible in FIG. **9**B and FIG. **9**B, has a diameter matching the interior diameter of the same matching commercial pipe. E.g., when connecting **24** to a ½ inch Schedule 40 PVC pipe, the matching dimensions for **51** would be a diameter of 21.33 mm and **52** would be a diameter of 15.80 mm. The bottom of **50** is visible in FIG. **9**D, which must be a smooth anti-static surface, like the other interior components of the helikon vortex.

FIGS. **10**A-**10**D are various views of a Wide Vortex Chamber Cap/Outlet Overview, with a front view (FIG. **10**A), top view (FIG. **10**B), top upper-front perspective view (FIG. **10**C), and lower-front perspective view (FIG. **10**D). The wide vortex chamber cap/outlet **37** is utilized in the unilateral compression helikon vortex, and the vortex output adapter **24** is visible in FIG. **10**A, FIG. **10**B, and FIG. **10**C. The top of the wide vortex chamber cap **53** is visible on FIG. **10**B and FIG. **10**C. To reduce helikon vortex manufacturing costs, the interior dimensions of the vortex output adapter **24** are intended to connect to commercial pipe with standard inner and outer diameters. The interior of vortex output adapter **51**, visible in FIG. **10**B, FIG. **10**C, and FIG. **10**D, has a diameter matching the outer diameter of a commercial pipe, while the vortex chamber cap outlet **52**, visible in FIG. **10**B and FIG. **10**D, has a diameter matching the interior diameter of the matching commercial pipe. E.g., when connecting **24** to a ½ inch Schedule 40 PVC pipe, the matching dimensions for **51** would be a diameter of 21.33 mm and **52** would be a diameter of 15.80 mm. The bottom of **53** is visible in FIG. **10**D, which must be a smooth anti-static surface, like the other interior components of the helikon vortex.

FIGS. **11**A-**11**C are various views of a Manually Calibrated Helikon Vortex Cone Overview, with a front view (FIG. **11**A), top view (FIG. **11**B), and lower-front perspective view (FIG. **11**C). The manually calibrated helikon vortex cone is one instantiation of **8** which can be utilized in either Bilateral or Unilateral Helikon Vortex configurations. The effective surface of the cone **54** is visible in FIG. **11**A, FIG. **11**B, and FIG. **11**C. This surface must be a smooth anti-static surface, like the other interior components of the helikon vortex. The base of the cone **55** is visible in FIG. **11**A and FIG. **11**C. In the center of the base of the cone is the threaded core of the cone **56** which is visible in FIG. **11**C. To reduce helikon vortex manufacturing costs, the threads are industry standard fine thread count and diameter so that the manually calibrated helikon vortex cone can be used with industry standard bold sizes. E.g., an industry standard ⅜" bolt size has a fine thread count of 24 threads per inch (TPI).

FIGS. **12**A-**12**B are various cross-sectional views of the Manually Calibrated Helikon Vortex Cone, with a Vertical Cross-Section View (FIG. **12**A) and a Horizontal Cross-Section View (FIG. **12**B). The effective surface of the cone **54** is visible in FIG. **12**A on the upper external surface of the vertical cross-section, while the base of the cone **55** is visible on the bottom. The effective surface of the cone **54** is visible in FIG. **12**B on the outer circumference of the horizontal cross-section. The threaded core of the cone **56** is visible on FIGS. **12**A and **12**B. To reduce helikon vortex manufacturing costs, the interior of the cone **57** is hollow, as seen on FIGS. **12**A and **12**B, precluding the utilization of unnecessary materials. The base of the cone is reinforced in three ways. First, a thick area of material reinforcement for the threaded core **58** is provided around **56**, as seen on FIGS. **12**A and **12**B. Second, radial reinforcement structures **59** and **60** extend from **58** (i.e., near the center of the cone) to **54** (i.e., the outside of the cone), as seen on FIG. **12**B. Third, and finally, a circular reinforcement structure **61** goes around the base of the cone and **56**, as seen on FIGS. **12**A and **12**B, connecting the inner radial reinforcement structures **59** to the outer reinforcement structures **60**. The inner and outer reinforcement structures, **59** and **60**, are distributed at even intervals of angles around the central axis of the cone, but the angles separating structures for **59** and **60** are not necessarily equal, as seen on FIG. **12**B, where six **59** are connected to **61** and eight **60** structures are connected to **61**. Larger cones may have multiple circular reinforcements **61**, in concentric circles, each connected by radial reinforcement structures, such as **59** or **60**, while smaller cones may not require a circular reinforcement structure **61** and only a single set of radial reinforcement structures, such as **59**, which would then directly connect **58** to **54**.

FIGS. **13**A-**13**C are various views of an Alternative Threaded Cone Overview, with a front view (FIG. **13**A), bottom view (FIG. **13**B), and lower-front perspective view (FIG. **13**C). The alternative threaded cone differs from the manually calibrated helikon vortex cone in FIGS. **11**A-**11**C in that it has no threaded core **56** and instead has a single threaded extrusion **62** and multiple axial alignment extrusions **63**, as seen on FIGS. **13**A, **13**B, and **13**C. The extrusions **62** and **63** are aligned with the central axis of the cone, with **62** being on the central axis as seen from the bottom view in FIG. **13**B. One or more axial alignment extrusions, **63**, appear around the central axis, with four visible on FIGS. **13**B and **13**C. The alternative threaded cone is intended for use with an electric motor **12** and the vortex exhaust/alternative threaded cone alignment base on FIGS. **15**A-**15**B and **16**A-**16**B.

FIGS. **14**A-**14**C are various views of a Vortex Exhaust/Cone Alignment Base Overview, with a front view (FIG. **14**A), top view (FIG. **14**B), and bottom view (FIG. **14**C). The vortex exhaust/cone alignment base **9** is utilized with the cone **8** illustrated in FIGS. **11A-11C** and has several critical functions. First, the bottom of the base **64**, visible on FIGS. **14A**, **14B** and **14C**, is held perpendicular to the central axis of the lower vortex chamber **7** via the connector to the vortex chamber **65**, visible on FIGS. **14A** and **14B**, which attaches to the lower narrow vortex chamber **33**. The inner diameter of **65** matches the outer diameter of **33** for alignment, and is large enough for the base of the cone **8** to be lowered into **9**. Second, two or more vertical vent fins **66**, visible on FIGS. **14A**, **14B**, and **14C**, are symmetrically distributed around the central axis of **9**, connecting **64** to **65**, while being tangential to airflow from **33**. The gaps between **66** permit exhaust to exit from the vortex chamber **9**. Third, the bottom of the base **64** is structurally reinforced to hold the cone **8** in alignment with the central axis of the lower vortex chamber **7** with one or more circular reinforcements **67**, visible on FIGS. **14A** and **14B**, symmetrically distributed radial reinforcements **68**, visible on FIG. **14B**, and a central reinforcement **69**, visible on FIG. **14B**, around the center of **64**. The structural reinforcements **67**, **68**, and **69** support the alignment of the cone **8** while precluding the utilization of unnecessary materials. At the top of the base, **65** is contoured to maximize surface area with **66** to add structural strength. The cone is held in place by a commercial hex that is inserted from the bottom of **64** into the cylindrical hollow central shaft of the base **70**, visible on FIGS. **14B** and **14C**. The hex head of the bolt fits into the base hex nut intrusion **71** which is visible on FIG. **14C**. Therefore, the manually calibrated helikon vortex cone **8**, in FIGS. **11A-11C**, can be attached to this vortex exhaust/cone alignment base **9**, in FIGS. **14A-14C**, with a commercial hex bolt. The cone can be lowered by turning it clockwise, from the top view, down onto the threaded bolt, and raised by turning it counter-clockwise. When the cone is in a lower position there is a larger gap between the cone **8** and the lower narrow vortex chamber **33**, allowing a larger volume of atmospheric gases to exhaust out of **7**. These exhaust gases, which exit below **65** on FIG. **14A** between the vent fins **66**, are the densest atmospheric gases, being on the outside perimeter of **7** while under centrifugal acceleration.

FIGS. **15A-15B** are various Perspective Views of the Vortex Exhaust/Cone Alignment Base, with an upper-front perspective view (FIG. **15A**) and a lower-front view perspective view (FIG. **15B**). All the reference numerals in FIGS. **14A-14C** are visible in FIGS. **15A-15B**. On FIG. **15A**, the circular and radial structural supports **67** and **68** can be seen to rise above the base **64**, providing reinforcement to **69**. The outermost circular structural support **67** also provides more surface area and structural support for **66** to attach to the base **64**. The intrusion for the hex bolt **71** can be clearly seen on FIG. **15B** in the center of the base **64**. The variable outer diameter of **65** can also be seen on FIG. **15B**, reducing materials required for construction while enhancing the surface are and structural support for **66** to attach to the connector **65**. The vortex exhaust/cone alignment base **9** utilizes a hex bolt held stationary in axial alignment by **69**, **70**, and **71**, and held in alignment with the lower narrow vortex chamber **33**, as seen on FIGS. 2A-2D and 3A-3D, by **65** and a plurality of **66**, while said hex bolt is threaded into cone **8** holding **8** in axial alignment by **56** and **58**, which are reinforced by **61** and a plurality of **59** and **60**, as seen on FIGS. **12A-12B**, while **8** can be rotated clockwise and counter-clockwise to raise and lower position of **8** inside **33**, constitutes a means to position said cone **8** inside said lower narrow vortex chamber **33**.

FIGS. **16A-16B** are various views of a Vortex Exhaust/Alternative Threaded Cone Alignment Base Overview, with a top view (FIG. **16A**), and bottom view (FIG. **16B**). The vortex exhaust/alternative cone alignment base **9** is utilized with the alternative threaded cone **8** illustrated in FIGS. **13A-13C** and differs by the vortex exhaust/cone alignment base **9** illustrated in FIGS. **14A-14C** in a few ways. First, instead of a smooth hollow central shaft **70**, this base has a threaded central shaft **72**, as seen on FIGS. **16A** and **16B**. Second, instead of the central reinforcement **69** being immediately around **70**, there is a circular central shaft **73** that can rotate clockwise and counter-clockwise, as seen on FIGS. **16A** and **16B**. Third, the central reinforcement for the base **69** goes around **73** in this configuration, as seen on FIG. **16A**. Fourth, there are axial alignment shafts **74** which extend through the radial reinforcements **68** and the base **64**, as seen on FIGS. **16A** and **16B**. The front view of this configuration of **9** appears to be the same as FIG. **14A**. The axial alignment extrusions **63** on the alternative threaded cone **8** extend through the axial alignment shafts **74** as the threaded extrusion **62** is threaded into **72**. Together, the alignment extrusions **62** and shafts **74** align the cone **8** with the vortex chamber **7**, as the cone position is raised and lowered by rotating **73** clockwise and counter-clockwise. Fifth, an axial alignment shaft reinforcement **75** is around each shaft **74** to reinforce the radial reinforcements **68**, as seen on FIG. **16A**. Finally, there is a motor attachment mount **76** on the bottom of **73**, as seen on FIG. **16B**. This is where an electrical motor **12** can be attached to rotate **73** to raise and lower the cone **8** via a control system **13** to automate the calibration process.

FIGS. **17A-17B** are Perspective Views of the Vortex Exhaust/Alternative Threaded Cone Alignment Base, with an upper-front perspective view (FIG. **17A**) and a lower-front view perspective view (FIG. **17B**). All the reference numerals in FIGS. **16A-16B** are visible in FIGS. **17A-17B**. On FIG. **17A**, the axial alignment shaft reinforcement **75** can be seen having a similar height to the radial, circular, and central reinforcement structures **67**, **68**, and **69**. The circular central shaft **73** can be seen extending from the center of **69** in FIG. **17A** to the center of **64** on FIG. **17B**, where the motor attachment mount **76** is located. The other functions of **64**, **65**, **66**, **67**, **68**, and **69** identified on FIGS. **15A-15B** above are applicable here. The vortex exhaust/alternative threaded cone alignment base **9** utilizes a threaded central shaft **72** that is held in axial alignment by **69** and **73**, and reinforced by a plurality of **68**, and held in alignment with the lower narrow vortex chamber **33**, as seen on FIGS. 2A-2D and 3A-3D, by **65** and a plurality of **66**, while **72** is threaded onto **62** of cone **8**, as seen on FIGS. **13A-13C**, holding **8** in axial alignment by a plurality of extrusions **63** which are inserted into **74**, which are reinforced by **68** and **75**, while **76** can be rotated clockwise and counter-clockwise manually or by an electric motor **12** to raise and lower the position of **8** inside **33**, constitutes a means to position said cone **8** inside said lower narrow vortex chamber **33**.

DRAWINGS—REFERENCE NUMERALS

1 helikon vortex
2 atmospheric gases
3 pressure sensor for atmospheric gases
4 CO_2 sensor for atmospheric gases
5 high-speed blower
6 airflow adapter
7 helikon vortex chamber
8 helikon vortex cone
9 helikon vortex exhaust/cone alignment base
10 dense molecular gas (vortex chamber exhaust)

11 low density molecular gas (vortex chamber product)
12 electrical motor
13 control system
14 relief control valve
15 relief valve gas output
16 relief valve output CO_2 sensor
17 vortex chamber control valve or controlled environment gaseous input control valve
18 vortex chamber control valve output
19 vortex chamber control valve output CO_2 sensor
20 controlled environment
21 pressure sensor for controlled environment
22 controlled environment gaseous output control valve
23 controlled environment exhaust
24 vortex output adapter
25 narrow vortex chamber cap/outlet
26 upper narrow vortex chamber
27 upper lateral vortex chamber adapter
28 blower input connector
29 radial to tangential airflow adapter
30 tangential airflow stabilizer
31 wide vortex chamber with tangential input
32 lower lateral vortex chamber adapter
33 lower narrow vortex chamber
34 interior cross-section area of tangential airflow stabilizer
35 excluded wedge from tangential airflow
36 reinforcement for the tangential airflow
37 wide vortex chamber cap/outlet
39 outer reinforcement for the tangential airflow
40 inner reinforcement for the tangential airflow
41 tangential airflow vent
42 narrow vortex chamber connector
43 wide vortex chamber connector
44 lateral adapter
45 interior of narrow vortex chamber connector
46 interior of wide vortex chamber connector
47 interior of lateral adapter
48 interior of narrow vortex chamber
49 exterior of narrow vortex chamber
50 narrow vortex chamber cap
51 interior of vortex output adapter
52 vortex chamber cap outlet
53 wide vortex chamber cap
54 effective surface of cone
55 base of cone
56 threaded core of cone
57 hollow interior of cone
58 reinforcement for threaded core of cone
59 inner radial reinforcement structure for cone
60 outer radial reinforcement structure for cone
61 circular reinforcement for cone
62 threaded extrusion
63 axial alignment extrusion
64 bottom of base
65 connector to vortex chamber
66 vent fin
67 circular reinforcement for base
68 radial reinforcement for base
69 central reinforcement for base
70 hollow central shaft
71 base hex nut intrusion
72 threaded central shaft
73 circular central shaft
74 axial alignment shaft
75 axial alignment shaft reinforcement
76 motor attachment mount

OPERATION

The operation for growing agricultural products with reduced ^{14}C content requires a controlled environment **20** with filtered atmospheric gases **2** from which CO_2 with ^{14}C has been removed.

1. A filtration system comprising a blower **5** and a helikon vortex **1** constitutes a means to remove CO_2 with ^{14}C from atmospheric gases **2**; blower **5** output velocity of 322 km per hour or greater is required for effective filtration with helicon vortex **1**;

2. Control valves **17**, **22** are required to control the flow of gases entering and exiting the controlled environment **20**;

3. When the CO_2 sensor **19** inside the controlled environment **20** detects a CO_2 abundance lower than a predetermined amount, the said filtration system is turned on by the control system **13** and the relief control valve **14** is opened;

4. The CO_2 sensor **16** at the relief output is monitored and compared to the CO_2 sensor **4** for atmospheric gases **2** outside the controlled environment to ensure said filtration system removal of CO_2 with ^{14}C from atmospheric gases **2** is effective by detecting a predetermined delta which can be determined by said filtration system efficiency;

5. Once effective filtration is verified, the control system **13** closes the relief control valve **14** and opens control valves **17**, **22** which are connected to the controlled environment **20**;

6. When the CO_2 sensor **19** inside the controlled environment **20** detects a CO_2 abundance above a predetermined amount, the said filtration system is turn off and the control valves **17**, **22** are closed by the control system **13**;

7. When the controlled environment input control valve **17** is open, the output control valve **22** is only opened by the control system **13** when the air pressure inside the controlled environment **20** as measured by the air pressure sensor **21** exceeds the atmospheric gas air pressure outside of the controlled environment by a predetermined amount as measured by air pressure sensor **3**;

8. Operation of said filtration system is initially required for a duration sufficient to replace the entire volume of air inside the controlled environment **20**. Thereafter, continuous, periodic, or intermittent operation as determined by CO_2 sensor **19**, as detailed above, may be used to determine periods of operation for the filtration system to maintain sufficient CO_2 levels inside the controlled environment **20**;

9. The control system **13** can either be programmed or configured to operate **5**, **14**, **17**, and **22** utilizing electronic controls or switches with digital or analog signals, constituting a means to operate the blower and control valves. Similarly, **13** can either be programmed or configured to monitor digital or analog signals from **3**, **4**, **16**, **19**, and **21**, constituting a means to monitor the sensors.

10. Helikon vortex **1** above may comprise either a bilateral compression helikon vortex or a unilateral compression helikon vortex as detailed below; effective filtration has been demonstrated with centrifugal acceleration exceeding 16,000 g, a maximum narrow vortex chamber radius of 5.08 cm, and a maximum height of 1.94 m.

11. Bilateral compression helikon vortex (FIG. **2**) consists of an airflow adapter **6** (consisting of blower input connector **28**, radial to tangential airflow adapter **29**, tangential airflow stabilizer **30**, and exclusion wedge **35**), vortex chamber **7** (consisting of a wide vortex chamber **31**, upper narrow vortex chamber **26**, lower narrow vortex chamber **33**, upper lateral adapter **27**, and lower lateral adapter **32**), cone **8**,

exhaust/cone alignment base **9**, vortex output adapter **24**, and narrow vortex chamber cap/outlet **25**;

12\. Unilateral compression helikon vortex (FIG. **3**) consists of an airflow adapter **6** (consisting of blower input connector **28**, radial to tangential airflow adapter **29**, tangential airflow stabilizer **30**, and exclusion wedge **35**), vortex chamber **7** (consisting of a wide vortex chamber **31**, lower narrow vortex chamber **33**, and lower lateral adapter **32**), cone **8**, exhaust/cone alignment base **9**, vortex output adapter **24**, and wide vortex chamber cap/outlet **37**;

13\. During operation, the atmospheric gases **2** are accelerated by blower **5** and enter the airflow adapter **6** were they are stabilized and shaped prior to tangential injection into the wide vortex chamber **31**; Centrifugal acceleration occurs while the atmospheric gases are separated by molecular density in vortex chamber **7**; after separation, the high-density gases exit **7** between **33** and **8**, while low-density gases exit **7** through **24**;

14\. Calibration of the helikon vortex is essential prior to operation and this is accomplished by adjusting the position of the cone **8** inside the narrow vortex chamber **33** to ensure effective separation of CO_2 with ^{14}C. For manual calibration, the vortex exhaust/cone alignment base **9** utilizes a hex bolt held stationary in axial alignment by **69**, **70**, and **71** (FIG. **15**), while cone **8** can be rotated clockwise and counter-clockwise to raise and lower the position of **8** inside **33**. Alternatively, the calibration process can be automated with an electric motor **12**. The vortex exhaust/alternative threaded cone alignment base **9** utilizes a threaded central shaft **72** that is held in axial alignment by **69** and **73** (FIG. **16**), holding **8** in axial alignment by a plurality of extrusions **63** (FIG. **13**) which are inserted into **74**, while **76** can be rotated clockwise and counter-clockwise by an electric motor **12** to raise and lower the position of **8** inside **33**.

REFERENCES CITED

U.S. Patent Documents

3,004,158	October 1961 Steimel, K.
3,421,334	January 1969 McKinney, et al. . . . 62-28
3,594,573	July 1971 Gerber, H.
3,925,036	December 1975 Shacter, J. . . . 55/158
3,939,354	February 1976 Janes, G. S. . . . 250/484
3,942,975	March 1976 Drummond, et al. . . . 75/10 R
4,070,171	January 1978 Wikdahl . . . 55/419
4,311,674	January 1982 Janner, et al. . . . 204/157.22
4,584,073	April 1986 Laboda, et al. . . . 204/157.2
4,638,674	October 1983 Redmann . . . 73/863.12
4,816,209	July 1986 Schweiger . . . 376/309
7,332,715 B2	February 2008 Russ, et al. . . . 250/288
8,460,434	June 2013 Turner, et al. . . . 95/117
9,579,666 B2	February 2013 Mangadoddy, et al. . . . B040C 5/04

OTHER PUBLICATIONS

Feiverson, H. A., Glaser, A., Mian, Z., & Von Hippel, F. N., Unmaking the Bomb: A Fissile Material Approach to Nuclear Disarmament and Nonproliferation, The MIT Press, Cambridge, Mass., London, England (2014).

Genome Reference Consortium (GRC) Human Genome Assembly build 38 (GRCh38), 24 Dec. 2013.

Lander, E. S. et al., Initial sequencing and analysis of the human genome, Nature 409, 860-921 (2001).

Moore, J. D. L., South Africa and Nuclear Proliferation, Palgrave Macmillan, New York, N.Y. (1987).

Patrick, A. D., & Patrick, B. E., Carbon 14 decay as a source of somatic point mutations in genes correlated with cancer diagnoses, Stable Isotope Foundation, Grants Pass, Oreg., USA (2017).

Purdom, C. E., Biological hazards of carbon-14, New Sci. 298, 255-257 (1962).

Sassi, M., et. al., Carbon-14 decay as a source of non-canonical bases in DNA, Biochimica et Biophysica Acta 1840 526-534 (2014).

Sender, R., Fuchs, S., & Milo, R., Revised estimates for the number of human and bacteria cells in the body, PLoS Biol 14(8): e1002533 (2016).

I claim:

1. A method of growing agricultural products with a reduced abundance of carbon-14 comprising:

a. providing a mixture of atmospheric gases with a measurable abundance of carbon dioxide and a measurable abundance of carbon dioxide with carbon-14;

b. removing, in a vortex chamber, carbon-dioxide with carbon-14 from said mixture of atmospheric gases;

c. a forcing, via a blower, said mixture of atmospheric gases through said vortex chamber to produce filtered atmospheric gases consisting of low density molecular gases;

d. venting, via an input control valve, airflow of said filtered atmospheric gases from said vortex chamber into a controlled environment having an airtight seal; and

e. outputting, via an output control valve, gasses from said controlled environment; further comprising verifying carbon-dioxide removal in said vortex chamber prior to venting, via the input control valve, airflow of said filtered atmospheric gases from said vortex chamber into said controlled environment; wherein verifying carbon-dioxide removal in said vortex chamber prior to venting, via the input control valve, airflow of said filtered atmospheric gases from said vortex chamber into said controlled environment includes: a. detecting, via a first carbon-dioxide sensor, carbon-dioxide abundance outside said controlled environment; b. detecting, via a second carbon-dioxide sensor, carbon-dioxide abundance in a relief output of said vortex chamber; d. comparing, via a control system, the detected carbon-dioxide abundance outside said controlled environment and the detected carbon-dioxide abundance in the relief output; and e. opening, via the control system, the input control valve when the detected carbon-dioxide abundance outside said controlled environment and the detected carbon-dioxide abundance in the relief output is at or above a predetermined delta.

2. The method according to claim **1**, further comprising regulating carbon-dioxide abundance in said controlled environment.

3. The method according to claim **2**, wherein regulating carbon-dioxide abundance in said controlled environment includes:

a. detecting, via a carbon-dioxide sensor, carbon-dioxide abundance in said controlled environment; and

b. controlling, via a control system, at least one of the input control valve, the output control valve, or the blower based on the detected carbon-dioxide abundance to maintain a predetermined carbon-dioxide abundance in said controlled environment.

4. The method according to claim **1**, further comprising maintaining a predetermined positive pressure into said controlled environment when said output control valve is opened or closed.

5. The method according to claim **4**, wherein maintaining a predetermined positive pressure into said controlled environment when said output control valve is opened or closed includes:

a. detecting, via an internal air pressure sensor, internal air pressure in said controlled environment;

b. detecting, via an external air pressure sensor, external air pressure of atmospheric gases outside said controlled environment; and

c. operating, via a control system, the input and output control valves to maintain the predetermined positive pressure into said controlled environment based on the detected internal and external air pressures.

6. The method according to claim **1**, wherein verifying carbon-dioxide removal in said vortex chamber prior to venting, via the input control valve, airflow of said filtered atmospheric gases from said vortex chamber into said controlled environment additionally includes:

a. detecting, via a third carbon-dioxide sensor, carbon-dioxide abundance in said controlled environment; and

b. opening, via the control system, a relief output control valve to provide the relief output from the vortex chamber when the detected carbon-dioxide abundance in said controlled environment is below a predetermined amount.

7. The method according to claim **6**, wherein verifying carbon-dioxide removal in said vortex chamber prior to venting, via the input control valve, airflow of said filtered atmospheric gases from said vortex chamber into said controlled environment further includes closing, via the control system, the relief output control valve when the detected carbon-dioxide abundance outside said controlled environment and the detected carbon-dioxide abundance in the relief output is below a predetermined delta.

* * * * *